DEVELOPMENT OF CELLULOSE-BASED HYDROGELS FROM POST-CONSUMER COTTON FABRICS FOR SUSTAINABLE FOOD COOLANT APPLICATIONS

By

Srividya Parthasarathy

Department of Food Science and Agricultural Chemistry

McGill University

Montreal, Canada

June 2024

A thesis submitted to McGill University in partial fulfillment of the requirements for the degree of Master of Science

TABLE OF CONTENTS

TABLE OF CONTENTS II

LIST OF FIGURES VII

LIST OF TABLES IX

ABSTRACT X

RÉSUMÉ XII

ACKNOWLEDGEMENTS XIV

CONTRIBUTION OF AUTHORS XV

PUBLICATIONS XVI

CONFERENCE PRESENTATION XVII

LIST OF ABBREVIATIONS XVIII

CHAPTER 1. INTRODUCTION 1

CHAPTER 2. LITERATURE REVIEW 4

- **2.1 ABSTRACT** 4
- **2.2 INTRODUCTION** 5
- **2.3 SYNTHESIS OF CELLULOSE HYDROGELS** 6
  - **2.3.1 Physical crosslinking of hydrogels** 8
    - *2.3.1.1 Freeze-thaw-induced crosslinking* 8
    - *2.3.1.2 Electrostatic interactions induced crosslinking* 10

2.3.2 Chemical crosslinking of hydrogels 11

2.3.2.1 Citric acid mediated crosslinking 11

2.3.2.2 Epichlorohydrin (ECH) mediated crosslinking 12

2.3.2.3 Glutaraldehyde-mediated crosslinking 13

2.4 APPLICATIONS OF CELLULOSE HYDROGELS IN FOOD INDUSTRY, WASTEWATER TREATMENT AND PURIFICATION, AND SUSTAINABLE AGRICULTURE 14

2.4.1 Food packaging 15

2.4.2 Food additive 18

2.4.3 Functional Foods 19

2.4.4 Water treatment and purification 21

2.4.5 Sustainable agriculture 22

2.5 CONCLUSIONS AND OUTLOOK 23

2.6 REFERENCES 25

CONNECTING STATEMENT I 37

CHAPTER 3. SUSTAINABLE AND ROBUST CELLULOSE-BASED CORE-SHELL HYDROGELS RECYCLED FROM WASTE COTTON FABRICS AS HIGH-PERFORMANCE FOOD COOLANTS 38

3.1 ABSTRACT 38

3.2 INTRODUCTION 39

3.3 RESULTS AND DISCUSSION 41

3.3.1 Cellulose-based hydrogel morphology 41

3.3.2 Cellulose-based hydrogel properties 43

3.3.2.1 Mechanical Properties 43

3.3.2.1 Water retention capacity on rehydration 45

3.3.2.3. Latent heat of fusion 47

3.3.3 Comparison study of conventional ice cubes and C2A10Cl hydrogels 48

3.4 CONCLUSION 49

3.5 EXPERIMENTAL SECTION 50

3.5.1 Materials 50

3.5.2 Preparation of cellulose-based hydrogels 50

3.5.3 Characterization 51

3.5.3.1 Cellulose-based hydrogel morphology 51

3.5.3.2 Cellulose-based hydrogel properties 51

3.5.4 Comparison study of conventional ice cubes and cellulose-based hydrogels 53

3.5.4.1 Thawing behavior 53

3.5.4.2 Cooling effect on blueberries 53

3.5.5 Statistical Analysis 53

3.6 REFERENCES 55

CONNECTING STATEMENT II 60

CHAPTER 4. DEVELOPMENT OF NOVEL ANTIBACTERIAL-INFUSED CELLULOSE HYDROGELS AS SUSTAINABLE FOOD COOLANTS FOR MICROBIAL CONTAMINATION REDUCTION 61

4.1 ABSTRACT 61

4.2 INTRODUCTION 62

4.3. MATERIALS AND METHODS 64

4.3.1 Reagents and Materials 64

4.3.2 Preparation of Antibacterial Hydrogels 64

4.3.3 Characterization 65

4.3.3.1 Cellulose Hydrogel Structure 65

4.3.3.1.1 Fourier transform infrared spectroscopy 65

4.3.3.1.2 Scanning electron microscope 65

4.3.3.2 Cellulose Hydrogel Properties 66

4.3.3.2.1 Mechanical strength 66

4.3.3.2.2 Water-retention capacity 66

4.3.4 Antibacterial assay 67

4.3.5 Statistical Analysis 67

4.4 RESULTS AND DISCUSSION 68

4.4.1 Cellulose Hydrogel Structure 68

4.4.1.1 Fourier transform infrared spectroscopy 68

4.4.1.2 Morphology 70

4.4.2 Cellulose Hydrogel Properties 71

4.4.2.1 Mechanical strength 71

4.4.2.2 Water retention capacity 73

4.4.3 Antibacterial Properties 74

4.5 CONCLUSION 76

4.6 REFERENCES 77

CHAPTER 5. A COMPREHENSIVE SCHOLARLY DISCUSSION OF ALL THE FINDINGS 86

CHAPTER 6. GENERAL SUMMARY AND CONCLUSION 90

6.1 GENERAL SUMMARY 90

6.2 SUGGESTIONS FOR FUTURE WORK 91

REFERENCES 92

LIST OF FIGURES

Figure 2.1 Applications of cellulose hydrogels in food-related industries.

Figure 2.2 Applications of cellulose-based hydrogels for (a) microbial inhibition, [52] (b) stabilization of Pickering emulsions, [53] (c) fat substitution, [54] (d) dye adsorption, [55] and (e) controlled release of fertilizers. [56]

Figure 3.1 SEM images of cross-sections of cellulose-based hydrogels before (upper) and after (below) five cycles of freeze-thaw treatment. *The dotted lines indicate the shell layers. Scale bar: 1 mm.

Figure 3.2 SEM images of surface morphology of cellulose-based hydrogels before (upper) and after (below) five cycles of freeze-thaw treatment. Scale bar: 1 mm.

Figure 3.3 Compressive stress-strain curves of cellulose-based hydrogels before and after freeze-thaw cycles: (A) C2A5Cl, (B) C2A10Cl, (C) CA2A5Cl, and (D) CA2A10Cl.

Figure 3.4 Water retention capacity on rehydration of cellulose-based hydrogels after freeze-thaw cycles. *Different letters on the top of columns represented the significant difference after freeze-thaw treatment ($p < 0.05$).

Figure 3.5 Latent heat of fusion (LHF) of cellulose-based hydrogels (A) before and (B) after 5 freeze-thaw cycles.

Figure 3.6 (A) Thawing curves and (B) cooling curves of conventional ice cubes and C2A10Cl hydrogels.

Figure 4.1 FTIR spectra of the dip-coated shell layer and core structures of CL, OXCL, OXCL-N, and OXCL-L hydrogels.

Figure 4.2 SEM images of cross-sections and surface morphology of OXCL, OXCL-N, and OXCL-L hydrogels before (upper) and after (below) five cycles of freeze-thaw treatment. *The doted lines indicate the shell layers, and the yellow marks represent deposition of nisin and lysozyme on their respective hydrogels. Scale bar: 1 mm.

Figure 4.3 Compressive stress-strain curves of antibacterial cellulose-based hydrogels before and after freeze-thaw cycles: (A) OXCL, (B) OXCL-N, and (C) OXCL-L hydrogels.

Figure 4.4 Compressive strength of antibacterial cellulose-based hydrogels before and after freeze-thaw cycles. *Different letters on the top of columns represents the significant difference between different samples for freeze-thaw treatments ($p < 0.05$).

Figure 4.5 Water retention capacity on rehydration of antibacterial cellulose-based hydrogels after freeze-thaw cycles. *Different letters on the top of columns represented the significant difference between different samples after freeze-thaw treatment ($p < 0.05$).

Figure 4.6 Antibacterial activity of OXCL-N (N), OXCL-L (L), and OXCL (NC) hydrogels against (A) *S. aureus* and (B) *E. coli.*

LIST OF TABLES

Table 2.1 Preparation methods and applications of recently reported cellulose hydrogels………...6

Table 3.1 Compositions of cellulose-based hydrogels…………………………………………...51

Table 4.1 Compositions of antibacterial cellulose-based hydrogels……………………………..65

ABSTRACT

In the past few decades, the textile industry has become very prominent, but it poses certain environmental challenges, including higher greenhouse gas emissions and leaching of toxic chemicals from waste accumulation and incineration processes. Cotton is a common material used in the textile industry, and recycling waste cotton fabrics is possible due to the cellulose-rich composition of cotton fibers. Cellulose is the most abundant natural polymer and an ideal candidate for the fabrication of hydrogels with robust mechanical strength, water retention capacity, and thermal stability. This study highlights the potential of employing cellulose-based hydrogels produced from waste cotton fabrics as a promising food coolant alternative with high compressive strength, good water retention property, high latent heat of fusion and reduced meltwater production in comparison to the conventional ice cubes, thus addressing the cross-contamination and food wastage problems. In Chapter 2, recent research on the development of cellulose-based hydrogels is reviewed with focus on the following aspects: (1) preparation of cellulose-hydrogels by physical and chemical crosslinking methods and (2) recent food-related applications of cellulose hydrogels in food packaging, food additives, functional foods, water treatment/purification and sustainable agriculture. Chapter 3 focused on the development of cellulose-based hydrogels with a special core-shell structure achieved by the dip-coating technique and investigated their structural, mechanical, water retention and thermal characteristics. Amongst the obtained hydrogels, the C2A10Cl hydrogel displayed the compressive strength of 144.7 kPa, high latent heat of fusion of 272.5 J/g, and water retention capacity of 72.2%. Moreover, the comparison studies revealed that the thawing curve of the C2A10Cl hydrogel showed a similar pattern to that of the conventional ice cubes while with no meltwater generation. The cooling performance of C2A10Cl hydrogels was comparable to conventional ice cubes using blueberries as a model, which were cooled from 22°C to 3.9°C in 32 minutes by C2A10Cl hydrogels and in 26 minutes by conventional ice cubes. Chapter 4 aimed to impart antibacterial property to the cellulose-based hydrogels to further ensure food safety. In this study, the ALG/$CaCl_2$ dip-coated oxidized cellulose hydrogels were developed using sodium periodate, and then chemically incorporated with antibacterial compounds, namely nisin and lysozymes. The hydrophilic nature of nisin and lysozyme remarkably improved the water retention capacities of both OXCL-N and OXCL-L hydrogels and contributed to a notable decrease in meltwater generation. The OXCL-N hydrogels demonstrated the highest compressive strength of 142.8 kPa. The antibacterial efficacy of the hydrogels was confirmed, as the OXCL-N and OXCL-L hydrogels displayed large inhibition zones of 3.66 mm and 4.06 mm against *S. aureus*, respectively, and slight inhibition effect against *E. coli*. Overall, this study presents a simple method for developing cellulose-based hydrogels with potential applications as sustainable food coolants.

RÉSUMÉ

Au cours des dernières décennies, l’industrie textile est devenue très importante, mais elle pose certains défis environnementaux, notamment des émissions de gaz à effet de serre plus élevées et le lessivage de produits chimiques toxiques provenant de l’accumulation de déchets et d’incinération. Le coton est un matériau couramment utilisé dans l'industrie textile, et le recyclage des déchets de tissus en coton est possible grâce à la composition riche en cellulose des fibres de coton. La cellulose est le polymère naturel le plus abondant et un candidat idéal pour la fabrication d’hydrogels dotés d’une résistance mécanique, d’une capacité de rétention d’eau et d’une stabilité thermique robustes. Cette étude met en évidence le potentiel de l'utilisation d'hydrogels à base de cellulose produits à partir de déchets de coton comme alternative prometteuse au liquide de refroidissement alimentaire avec une résistance élevée à la compression, une bonne propriété de rétention d'eau, une chaleur latente de fusion élevée et une production réduite d'eau de fonte par rapport aux glaçons conventionnels, donc résolvant ainsi les problèmes de contamination croisée et de gaspillage alimentaire. Dans le chapitre 2, les recherches récentes sur le développement d'hydrogels à base de cellulose sont passées en revue en mettant l'accent sur les aspects suivants : (1) préparation d'hydrogels de cellulose par des méthodes de réticulation physiques et chimiques, et (2) applications récentes des hydrogels de cellulose dans les domaines de l'emballage alimentaire, des additifs alimentaires, des aliments fonctionnels, du traitement/purification de l'eau et de l'agriculture durable. Le chapitre 3 s'est concentré sur le développement d'hydrogels à base de cellulose avec une structure noyau-coquille spéciale obtenue par la technique de revêtement par immersion et a étudié leurs caractéristiques structurelles, mécaniques, de rétention d'eau et thermiques. Parmi les hydrogels obtenus, l'hydrogel C2A10Cl présentait une résistance à la compression de 144,7 kPa, une chaleur latente de fusion élevée de 272,5 J/g et une capacité de

rétention d'eau de 72,2 %. De plus, les études comparatives ont révélé que la courbe de décongélation de l'hydrogel C2A10Cl présentait un schéma similaire à celui des glaçons conventionnels, sans génération d'eau de fonte. Les performances de refroidissement des hydrogels C2A10Cl étaient comparables à celles des glaçons conventionnels utilisant les myrtilles comme modèle, qui ont été refroidies de 22°C à 3,9°C en 32 minutes par des hydrogels C2A10Cl et en 26 minutes par des glaçons conventionnels. Le chapitre 4 visait à conférer des propriétés antimicrobiennes aux hydrogels à base de cellulose afin de garantir davantage la sécurité alimentaire. Dans cette étude, les hydrogels de cellulose oxydée recouverts d'ALG/CaCl2 ont été développés à l'aide de périodate de sodium, puis incorporés chimiquement à des composés antimicrobiens, à savoir la nisine et les lysozymes. La nature hydrophile de la nisine et du lysozyme a remarquablement amélioré les capacités de rétention d'eau des hydrogels OXCL-N et OXCL-L et a contribué à une diminution notable de la production d'eau de fonte. Les hydrogels OXCL-N ont démontré la résistance à la compression la plus élevée de 142,8 kPa. L'efficacité antimicrobienne des hydrogels a été confirmée, car les hydrogels OXCL-N et OXCL-L présentaient de grandes zones d'inhibition de 3,66 mm et 4,06 mm contre S. aureus, respectivement, et un léger effet d'inhibition contre E. coli. Dans l'ensemble, cette étude présente une méthode simple pour développer des hydrogels à base de cellulose avec des applications potentielles comme liquides de refroidissement alimentaires durables.

ACKNOWLEDGEMENTS

I am deeply grateful for the immense support and assistance I have received throughout the process of writing this dissertation.

First and foremost, I want to express my deep gratitude to my supervisor, Dr. Yixiang Wang for his exceptional mentorship throughout my thesis by providing me with constructive feedback that has helped me refine my work. I am truly appreciative of his willingness to share his extensive knowledge with me, as well as for encouraging me to explore new perspectives, which greatly contributed to the formulation of this thesis.

A special acknowledgement is extended to all the members of Dr. Wang's lab, including Shuting Huang, Yirong Zhang, Kehao Huang, Chuye Ji, Hussein Mostafa, Negar Haghighatpanah, Yaqi Chu, Jiachen Wei, and Yuqi Tong. Each of their collaborative support has been greatly appreciated.

Furthermore, I am immensely grateful to my parents and my brother for their unwavering love, emotional support and prayers. They have been a constant source of comfort and encouragement, and I am truly blessed for their presence in my life.

I also wish to express my gratitude to my dearest friends, Saleth Sidharthan, Sanjeev Ganesh, Taranum Fathima Ali Y and Thamizhvani K from whom I derived lots of strength and inspiration. They have consistently been there for me; their companionship and insightful discussions have enriched both my academic and personal experiences over the years.

CONTRIBUTION OF AUTHORS

This thesis is edited in a manuscript format and consists of five chapters.

Chapter 1 presents a general introduction that includes a brief overview of the recent relevant work in literature and describes the research objectives in the thesis. Chapter 2 provides an overview of cellulose hydrogels, highlighting their preparation methods and potential applications in food industry, wastewater treatment, and agricultural sectors, and outlining areas for future research. Chapter 3 presents the development of cellulose-based hydrogels with a distinctive core-shell design that possess high mechanical strength, good water retention capacity, and comparable latent heat of fusion to conventional ice cubes and are suitable for food cooling purposes. Chapter 4 demonstrates the structure, mechanical properties, water retention property, and antibacterial efficacy of the oxidized cellulose hydrogels with the incorporation of antibacterial compounds. Chapter 5 carries out a comprehensive scholarly discussion of all the findings. Finally, Chapter 6 presents the overall conclusion of the thesis, as well as some suggestions for future research.

The present author, Srividya Parthasarathy, was responsible for the experimental work, data acquisition and formal analysis, validation and writing of the thesis. Dr. Yixiang Wang, the thesis supervisor, guided the research and revised the thesis before submission. Kehao Huang was partly responsible for the review and revision of Chapter 2. In Chapter 3, Yirong Zhang was partly responsible for validation and review of the experimental and written work. In Chapter 4, Kehao Huang was responsible for conducting the experimental part of the antibacterial assay.

PUBLICATIONS

Parthasarathy, S., Zhang, Y., & Wang, Y. “Sustainable and robust cellulose-based core-shell hydrogels recycled from waste cotton fabrics as high-performance food coolants”, Advanced Sustainable Systems, submitted in May 2024.

Parthasarathy, S., Huang, K., & Wang, Y. “Development of novel antibacterial-infused cellulose hydrogels as sustainable food coolants for microbial contamination reduction”, to be submitted.

CONFERENCE PRESENTATION

Parthasarathy, S., Zhang, Y., & Wang, Y. “Sustainable and robust cellulose-based core-shell hydrogels recycled from waste cotton fabrics as high-performance food coolants”, Future of Food Symposium, Montreal, May 2024 (poster presentation).

Parthasarathy, S., Zhang, Y., & Wang, Y. “Sustainable and robust cellulose-based core-shell hydrogels recycled from waste cotton fabrics as high-performance food coolants”, CSC 2024, Winnipeg, June 2024 (poster presentation).

LIST OF ABBREVIATIONS

ALG:	Alginate
ALG/$CaCl_2$:	Alginate/Calcium Chloride
$CaCl_2$:	Calcium chloride
Citric Acid:	CA
C2A5Cl:	100% Cellulose- Dip coated in 2%- alginate and 5%- calcium chloride
C2A10Cl:	100% Cellulose- Dip coated in 2%- alginate and 10% - calcium chloride
CA2A5Cl:	80:20%-Cellulose/Alginate- Dip coated in 2%- alginate and 5% calcium chloride
CA2A10Cl:	80:20%-Cellulose/Alginate- Dip coated in 2%- alginate and 10% calcium chloride
CL:	Cellulose
CL/ALG:	Cellulose/Alginate
CMC:	Carboxymethyl Cellulose
CMCF:	Carboxymethyl Cellulose Nanofibril
CNC:	Cellulose Nanocrystals

DSC:	Differential Scanning Calorimetry
ECH:	Epichlorohydrin
FT:	Freeze-thaw
FT0:	Freeze-thaw cycle 0
FT1:	Freeze-thaw cycle 1
FT5:	Freeze-thaw cycle 5
FTC:	Freeze-thaw cycles
FTIR:	Fourier transform infrared spectroscopy
FTT:	Freeze-thaw treatment
LHF:	Latent heat of fusion
NaOH/Urea:	Sodium Hydroxide-Urea
OXCL:	Oxidized cellulose
OXCL-L:	Oxidized cellulose- Lysozyme
OXCL-N:	Oxidized cellulose- Nisin
PVA:	Polyvinyl Alcohol
SEM:	Scanning Electron Microscopy
TOCNFs:	TEMPO-oxidized CNF

TSA:	Trypic Soy Agar
TSB:	Trypic Soy Broth
ZnO:	Zinc Oxide

CHAPTER 1. INTRODUCTION

The textile industry is one of the oldest, tracing back to 5000 B.C. with multifaceted production sectors primarily occupied by small-scale enterprises [1,2]. In recent years, the textile industry has experienced a drastic increase in clothing production and consumption, due to the increasing population and high global demand [3]. Since the ancient era, there has been a high utilization of natural fibers as a source of raw materials in the textile manufacturing industry [4]. Compared to 1995-1996, there has been a higher utilization (70%) of cotton in 2017-2018, with a remarkable inclination of 75.86% towards its production, import, and export in the last 23 years. [5]. However, the clothing sector is a primary cause of soil pollution from the landfill accumulation, and its incineration causes nearly 2-8% of annual greenhouse gas emissions, [6] such as methane (50%) and carbon dioxide (45%), leading to global warming and air pollution [7]. Hence, the textile industry is positioned as the second-largest contributor to carbon emissions of about 10% globally, with high wastewater effluent generation [8-10]. A statistical analysis by the World Bank has predicted a 70% increase in global municipal solid waste, escalating from 1.3 to 2.2 billion tons annually by 2025 [11]. A substantial percentage of waste textiles are disposed of in landfills, with only 15% being recycled. [12]. As mentioned above, the lack of efficient waste management poses a significant environmental issue, creating health hazards, hence, effective handling of cotton textile waste is essential. Cotton is known for its high cellulose content (approximately 95%), which has a linear polysaccharide chain of β $(1 \rightarrow 4)$ linked d-glucose units [13,14]. Cellulose can be obtained from many renewable sources and has great advantages such as biodegradability and eco-friendliness, and is known to be one of the safest materials [15]. The unique features of cellulose include the presence of numerous hydroxyl groups, high hydrophilicity, and adjustable properties in response to pH, time, temperature, and chemical reactions [16]. This renders cellulose an attractive choice for various hydrogel-related applications, thereby serving as an efficient strategy for recycling the waste cotton textiles and reducing environmental pollution.

Temperature conditions significantly influence the quality of chilled and perishable food products. Frequent unexpected temperature changes may occur in the food supply chain, jeopardizing consumer confidence and increasing food wastage [17]. Mismanagement of temperature in the food chain has evidenced substantial food loss and wastage, estimated at up to 35% [18]. In the developed nations, nearly 22% of food ends up as household waste [19]. According to the United Nations Environment Program's Food Waste Index Report, about 931 million tons of food waste was generated in 2019 [20]. The FDA's food code mandates foods to be stored at or below 41 °F (5 °C), as the high temperature can result in poor food quality and increased food safety risks and wastage due to the increased enzymatic and microbial activity [21]. Microorganisms responsible for foodborne illnesses are stated to multiply within the temperature range of 5 °C to 57 °C, [22] with elevated temperatures fostering rapid bacterial proliferation [23]. Particularly, Staphylococcus aureus (*S. aureus*), a gram-positive bacterium, is one of the most common foodborne pathogens. *S. aureus* is estimated to cause nearly 241,000 illness cases annually in the United States [24]. Moreover, Escherichia coli (*E. coli*) is a major bacterium causing foodborne infections, prevalent in food and environmental samples [25,26]. In 2020, an outbreak of Shiga toxin-producing *E. coli* occurred in Germany, with 3,785 illness cases reported and linked to contamination of sprouted seeds [27].

Over the years, conventional water-based ice cubes have been widely employed to maintain the temperature of food products, valued for their cost-effectiveness, efficiency, and convenience [28]. However, they hold certain disadvantages that warrant consideration of their usage such as the generation of meltwater from the ice cubes, causing microbial cross-contamination of food products and leading to substantial food loss and wastage [29]. Moreover, they aggravate excessive utilization of water resources and plastic packaging, posing a major environmental threat [30]. There has been exploration for alternatives such as antibacterial stoned-based and certain hydrogel-based coolants, but due to their own limitations, an inevitable requirement exists for the development of an efficient and cost-effective coolant system without any compromise in food safety and cooling efficiency.

To summarize, the purpose of this study is to develop an environment-friendly cellulose-based hydrogel from waste cotton as a sustainable and robust food coolant. The two main objectives of this study include: (1) To develop cellulose-based hydrogels from waste cotton fabrics with a unique core-shell structure and investigate their properties and cooling performance; and (2) To impart antibacterial property to the cellulose-based hydrogels and study their mechanical strength, water retention, and antibacterial effectiveness against *S. aureus* and *E. coli*.

CHAPTER 2. LITERATURE REVIEW

2.1 ABSTRACT

Hydrogels are three-dimensional crosslinked materials whose versatile applications have attracted the attention of food industry. Cellulose is the most abundant natural organic polymer on earth. It is inexpensive, biodegradable, and non-toxic, and has excellent mechanical properties and adjustable hydrophilicity, making it a potential material for constructing hydrogels. Feasible methods of fabricating cellulose hydrogels can be classified as physical crosslinking and chemical crosslinking methods. The resultant cellulose hydrogels have been used for food packaging, food additives, functional foods, wastewater treatment, and sustained agriculture. This review provides an overview of the fabrication of cellulose hydrogels, their applications in food and agriculture, and the prospective avenues and opportunities for future research.

Keywords: Hydrogel; Cellulose; Crosslinking; Food; Applications.

2.2 INTRODUCTION

Hydrogels are a three-dimensional network that can absorb large amounts of water. The first attempt at synthesizing hydrogels was reported in 1960 for use as soft contact lenses [1]. Nowadays, they are valued for their versatility and easy preparation in industrial applications including biosensors, wound dressing, drug delivery, surface coating, cosmetics, personal care, water purification, food, etc. [2,3]. Recently, hydrogels made from biomaterials have been proposed as a solution to the problem of environmental pollution caused by conventional plastics. For such applications, various biopolymers such as cellulose, chitosan, gelatin, and carrageenan have been explored to produce hydrogels [4].

Cellulose, being one of the most common natural polysaccharides, is predominantly found in plants, animals, and some bacteria. It has drawn a lot of attention as a food supplement due to its abundance, biodegradability, non-toxicity, and excellent mechanical properties [5]. The development of various cellulose solvents including *N*-methylmorpholine-*N*-oxide, Lithium chloride/N,N-Dimethylacetamide, ionic liquids, alkali/urea solutions, etc, has led to an efficient and environmentally friendly method of dissolving cellulose and producing cellulose-based hydrogels [6]. In recent years, cellulose-based hydrogels have been synthesized using cellulose and/or its derivatives such as carboxymethyl cellulose (CMC), hydroxypropyl cellulose, hydroxypropylmethyl cellulose, and methyl cellulose [7]. Compared with other biopolymer-based hydrogels, cellulose-based hydrogels have numerous striking features including good swelling ability, flexibility, and responsiveness to time, pH, and temperature [8]. According to the Web of Science search result, 3,565 research papers on cellulose-based hydrogels have been published from 2018 to 2023, with applications in biomedicine, agriculture, water purification, tissue engineering, batteries, etc., but only 400 (11.22%) of them are related to food applications. The development of cellulose-based hydrogels for food packaging and food additives is promising and has a huge potential. Several reviews have summarized the concepts, classifications, and preparation methods of cellulose-based hydrogels, but without the focus on food related applications [9,10]. Therefore, this review focuses on recent advances in cellulose hydrogels and presents the preparation of cellulose-based hydrogels by physical and/or chemical crosslinking methods, as well as recent applications of cellulose-based hydrogels in the food-related sectors.

2.3 SYNTHESIS OF CELLULOSE HYDROGELS

The synthesis of cellulose-based hydrogels can be achieved by physical and chemical crosslinking methods. The hydrogels crosslinked by physical interactions are based on reversible non-covalent bonds such as hydrophobic interactions, hydrogen bonds, van der Waals forces, and chain entanglements [9,11]. On the other hand, the chemical crosslinking of hydrogel is based on the addition of crosslinkers such as esterifying agents and etherifying agents to form -COOR and R-C-R moieties, respectively, leading to an irreversible network [12]. The preparation methods of recently reported cellulose hydrogels are summarized in Table 2.1.

Table 2.1 Preparation methods and applications of recently reported cellulose hydrogels

Materials	Preparation methods	Applications	Major Properties	Refs
CMC/gelatin	Glutaraldehyde as a crosslinker	Food packaging	Improved thermal stability and mechanical properties. High antibacterial and antioxidant properties.	[13]

CMC	Freeze-thaw induced crosslinking	Food packaging	Excellent stretchability, adhesion, self-healing, UV shielding, gas barrier properties, antioxidant, and antibacterial properties.	[14]
Alginate/CMC	Free radical polymerization	Nutrients delivery	Increased drug diffusion resistance, delayed drug release, and good stability.	[15]
Starch/magnetite /CNC	Radical polymerization	Wastewater purification	Improved salt sensitivity and thermal and magnetic properties.	[16]
Cellulose/bentonite	Epichlorohydrin as a crosslinker	Sustained agriculture	Improved textural properties and water retention capacities.	[17]
CMC/polyacrylamide	Methylene bisacrylamide as a crosslinker	Wastewater purification	Superior adsorption capacity and catalytic activity.	[18]
CMC	Citric acid as a crosslinker	Nutrients delivery	Maintained water absorption, delayed thermal degradation, enhanced thermal stability, and no phytotoxicity.	[19]
Cellulose	Carbodiimide as a crosslinker	Sustained agriculture	Increased water retention capability of the soil. Sustained	[20]

			release of water to the plants for a longer time.	
Cellulose	Glycine as a crosslinker	Wastewater purification	Enhanced swelling, mechanical strength, porosity, stability, thermodynamic durability, and reusability.	[21]
CMC/tamarind gum	Citric acid as a crosslinker	Functional foods	High antioxidant property.	[22]
Methylcellulose	Citric acid as a crosslinker	Functional foods	Improved barrier properties. Less affinity for water.	[23]

2.3.1 Physical crosslinking of hydrogels

Physical interactions such as hydrogen bonds and electrostatic interactions have drawn much attention in food industry due to their ability to induce crosslinking of hydrogels without the need for any catalysts or chemical crosslinkers. Appropriate selection of the hydrocolloid type, polymer concentration, and pH is essential, as it leads to the development of a wide variety of hydrogels.

2.3.1.1 Freeze-thaw-induced crosslinking

Freeze-thaw process comprises a series of cycles of freezing and thawing that result in the formation of microcrystals of frozen solvent and the crosslinked insoluble polymer chains, leading to a crosslinked hydrogel with elastic and porous characteristics. The processing parameters including thawing time, temperatures, freeze-thaw cycles, and the concentration of polymers determine the properties of the produced hydrogels [24]. The increased freezing time and the number of cycles were reported to enhance the formation of the crosslinked network and improve the mechanical properties of the hydrogels. However, the optimal freezing time for the different cellulose hydrogels should be determined case by case to avoid excessive growth of ice crystals, which could lead to a reduction in mechanical strength [25].

Sekine et al. prepared CMC nanofiber (CMCF) hydrogels by freezing CMCF solutions at -20 °C for 12 hours and then thawing at -4 °C for 12 hours [26]. The resultant hydrogels had a rigid porous structure with a pore diameter of approximately 80 µm, water content of >94%, compressive strength of >80 MPa, and strain of about 80% after three cycles of compression tests. Besides, the faster freezing process led to a higher compressive strength but lower compressive recovery of the produced hydrogels, which was attributed to the different sizes of ice crystals. Liu et al. fabricated a hydrogel based on cellulose nanocrystals (CNC), xylan, and polyvinyl alcohol (PVA), which was frozen at -20 °C for 12 hours, thawed at room temperature for 1 hour, and repeated twice [27]. During the freeze-thaw process, an irreversible crosslinked structure was formed between the PVA molecules with the microcrystalline structure as the crosslinking point, and the increased concentration of PVA (20 wt%) formed the denser network structure of the hydrogels, resulting in the improved mechanical properties and reduced swelling ratio. The maximum compressive strength and strain of the nanocomposite hydrogel were 1.56 MPa and 771%, respectively, and its swelling rate was 3.41 g/g. Moreover, abundant uncrosslinked hydroxyl groups within the hydrogel formed reversible crosslinking through hydrogen bonding after the thawing process, which enabled the hydrogel to be self-healable with a self-healing efficiency of approximately 25%. A highly stretchable hydrogel film with a thickness of 550-600 µm and a honeycomb internal structure was prepared by Zhao et al. using CMC, PVA, poly(ethylene imine), and tannic acid frozen at -20 °C for 12 hours and then thawed at room temperature [14]. The incorporation of 0.6%

of tannic acid led to a maximum tensile stress of 502.12 kPa and a strain of 397.65% of hydrogel film with about 100% UV-shielding ability.

2.3.1.2 Electrostatic interactions induced crosslinking

The gelation of polyelectrolyte solutions with oppositely charged multivalent ions is the main principle for the fabrication of crosslinked hydrogels based on electrostatic interactions [9]. Cellulose with highly reactive hydroxyl groups on the surface has gained great interest in the modification of cellulose into charged derivatives such as CMC and quaternized cellulose to form polyelectrolytes [28]. These polyelectrolyte complexes can be modified by various factors such as the quantity and ratio of the polymers used, charge density, and the net charge of the complex that influences its solubility and precipitation. Tuan Mohamood et al. produced a CMC-based hydrogel from biomass waste of oil palm empty fruit bunch using $CaCl_2$ as the crosslinking agent and investigated the effect of CMC concentration, $CaCl_2$ concentration, and reaction times on the properties of hydrogels [29]. The authors suggested 20% (w/v) of CMC as the optimal concentration to obtain the highest gel content of 28.11% with the lowest swelling ratio of 46.78 g/g. However, $CaCl_2$ with a concentration above 1% (w/v) caused decreased flexibility and aggregation of CMC chains. Li et al. synthesized a semi-interpenetrating hydrogel based on Krasch polysaccharide and CNC crosslinked by ferric ions [30]. The incorporation of CNC into the polysaccharides reinforced the rigidity of the network, leading to improved fracture strength of 2449.40 Pa and decreased swelling ratio of 21.17 g/g. An antimicrobial CMC hydrogel crosslinked by divalent zinc ions and incorporated with zinc oxide nanoparticles was manufactured by Priyadarshi et al [31]. CMC served as a matrix of the hydrogel and was crosslinked with Zn^{2+}. The pH of the reaction mixture was increased to 8.5, leading to the precipitation of zinc hydroxide and the formation of zinc oxide nanoparticles under heating process. The resultant CMC/zinc oxide hydrogel had around 2,800% water absorption capacity and excellent antibacterial efficacy against *L. monocytogenes* and *E. coli* after 12 hours of exposure.

2.3.2 Chemical crosslinking of hydrogels

In the chemical crosslinking method, covalent bonds between polymer chains are induced to develop a permanent hydrogel, where there is an addition of small crosslinker compounds or by inducing enzyme-catalyzed reactions [32]. The most used crosslinking agents are citric acid, epichlorohydrin, and glutaraldehyde [33]. To enhance crosslinking efficiency, optimize the characteristics of crosslinked materials, assess the long-term performance and stability of materials, and investigate new applications, the following factors such as alterations in crosslinking conditions and mixed crosslinking agents could be considered to take the merit of positive features of each crosslinker. In general, hydrogels generated via chemical crosslinking have stronger mechanical characteristics, greater stability, and longer durability, in comparison with the physically crosslinked hydrogels. However, it is also important to consider their biodegradability and behavior in the environment after they are discarded [34].

2.3.2.1 Citric acid mediated crosslinking

Citric acid (CA) is a polycarboxylic acid with three hydroxyl groups extracted from citrus fruits. It has advantages such as inexpensiveness, nontoxicity, hydrophilicity, and the ability to form strong hydrogen bonds to enhance thermal and water stability [35]. CA can stabilize cellulose hydrogels by forming covalent intermolecular di-ester bonds with the hydroxyl groups of cellulose. With all these attractive features, CA has been established as a cross-linking agent in the formation of cellulose hydrogels that have been designated as safe to use by the Food and Drug Administration. CA has been widely employed in food industry as a food additive and has anticoagulant and antiviral properties [36]. Nguyen et al. fabricated a gellan gum/cellulose/polyethylene glycol (PEG) hydrogel crosslinked with CA and investigated the effect of component concentration on the properties of hydrogels [37]. It was mentioned that the crosslinking of the polymer matrix did not significantly contribute to the final mechanical integrity of the hydrogels due to the acid-catalyzed depolymerization. However, the addition of PEG increased the number of hydroxyl groups and enhanced the bonding with CA groups, thus, improving the ex-situ crosslinking and mechanical properties of the materials. Moreover, the highest swelling ratio (around 750%) of hydrogel was found at 5% CA compared to 10% and 15% CA, which was attributed to excess crosslinking at high concentrations. Similar results were found in the hydrogel constructed from CMC and poly(ethylene oxide), where 10% CA was found to be the optimal concentration to obtain the highest swelling ratio (25%) of the hydrogel [38]. In addition, the curing temperature and time are adjusted to 70 °C and 150 minutes, respectively, to prevent the destruction of the hydrogel and to obtain the highest swelling rate. Lungu et al. compared the nanocellulose-based hydrogel crosslinked by CA and Ca^{2+} [39]. The hydrogel stabilized by CA had a highly porous structure and Ca^{2+}-crosslinked hydrogel showed internal laminar structuring, separated by generous interlayer spaces. Besides, CA-crosslinked hydrogel had better gel fraction, swelling ratio, and elasticity compared to Ca^{2+}-crosslinked one.

2.3.2.2 Epichlorohydrin (ECH) mediated crosslinking

The reaction between cellulose and epichlorohydrin (ECH) is generally catalyzed by a base, and the mechanism is governed by both physical and chemical interactions, where both ether bond formation and chain entanglement occur simultaneously [40]. ECH regulates the degree of swelling of hydrogels while modulating other mechanical qualities like compressive strength. It is generally known that viscosity increases with the increase in resistance to the motion of molecules, showing a relationship between viscosity and the quantity of cross-linking in the network [9]. The double crosslinking technique has been proven to be successful in mitigating the negative effects. Han et al. prepared a CMC/polyacrylamide hydrogel, and the addition of ECH decreased the density of the hydrogels from 0.25 ± 0.02 cm^3/g to 0.14 ± 0.01 cm^3/g, leading to denser and smoother surface texture, and the compression force was enhanced from 23 kPa to 70 kPa [41]. Chen et al. constructed a cellulose-based hydrogel by dissolving cellulose and sodium alginate in NaOH/urea solution, followed by cross-linking with ECH in the presence of attapulgite at 50 ℃ for 4 hours [42]. The nanocomposite hydrogel had the porous structure and rough inner surface morphology. Besides, the swelling degree of nanocomposite hydrogel increased from 36.9 times to 42.8 times with the increase of sodium alginate, and the incorporation of attapulgite enhanced the dye adsorption capacity in comparison with the hydrogels without attapulgite to 24.3 mg/g. Nguyen et al. proposed a facial method to synthesize the cellulose hydrogels based on direct dissolution of cellulose in tetrabutylphosphonium hydroxide followed by ECH crosslinking [43]. Increasing cellulose concentrations and ECH ratio resulted in shorter gelation time and stronger and stiffer hydrogels, which were due to the higher chemical crosslinking density. The highest compressive stress (44.02 kPa) was found in the hydrogel with 10% cellulose and 3% ECH.

2.3.2.3 Glutaraldehyde-mediated crosslinking

Glutaraldehyde has been used as a crosslinking agent as it is inexpensive, easy to process, less toxic, and highly soluble and reactive [9], and can react with the hydroxyl groups of cellulose [44]. The efficacy of glutaraldehyde crosslinking is influenced by reaction temperature and crosslinker concentration. For instance, Rana et al. revealed the effect of glutaraldehyde concentration on the properties of cellulose acetate/acrylic acid hydrogel [45]. It was showed that 30×10^{-2} mol/L of glutaraldehyde was optimal to obtain the highest grafting percentage (141.5%) of hydrogel, and increased crosslinker content contributed to a decrease in grafting rate, as the high concentration of crosslinker provided toughness and stiffness to the polymer structure. Wahid et al. developed a bacterial cellulose/chitosan-based semi-interpenetrating hydrogels by crosslinking with glutaraldehyde [46]. Both pure bacterial cellulose and chitosan hydrogels had weak mechanical properties, but the composite hydrogels with connections between the cellulose and chitosan networks showed better stability. By lowering the ratio of cellulose to chitosan, the structure of hydrogel became denser, and the storage modulus increased to about 3,850 Pa. The increased cellulose concentration limited the miscibility of the polymer in the chitosan network. However, a common problem with using glutaraldehyde as a crosslinker is its potential toxicity. The removal of possible residues after the reaction must be carefully considered. To address this issue, various strategies have been developed to minimize the cytotoxicity such as decreasing the concentration that led to the reduced efficiency of crosslinking and adding molecules that have the capacity to bind with the excessive unreacted glutaraldehyde molecules.

2.4 APPLICATIONS OF CELLULOSE HYDROGELS IN FOOD INDUSTRY, WASTEWATER TREATMENT AND PURIFICATION, AND SUSTAINABLE AGRICULTURE

The applications of hydrogels are widespread in the food, biomedical, cosmetic, and pharmaceutical industries. Due to its unparalleled properties such as unique surface characteristics, high mechanical strength, adjustable hydrophilicity, and ease of production, researchers are currently developing cellulose hydrogels for various food related applications such as food packaging, emulsion stabilizers, functional foods, and sustainable agriculture, as shown in Figure 2.1.

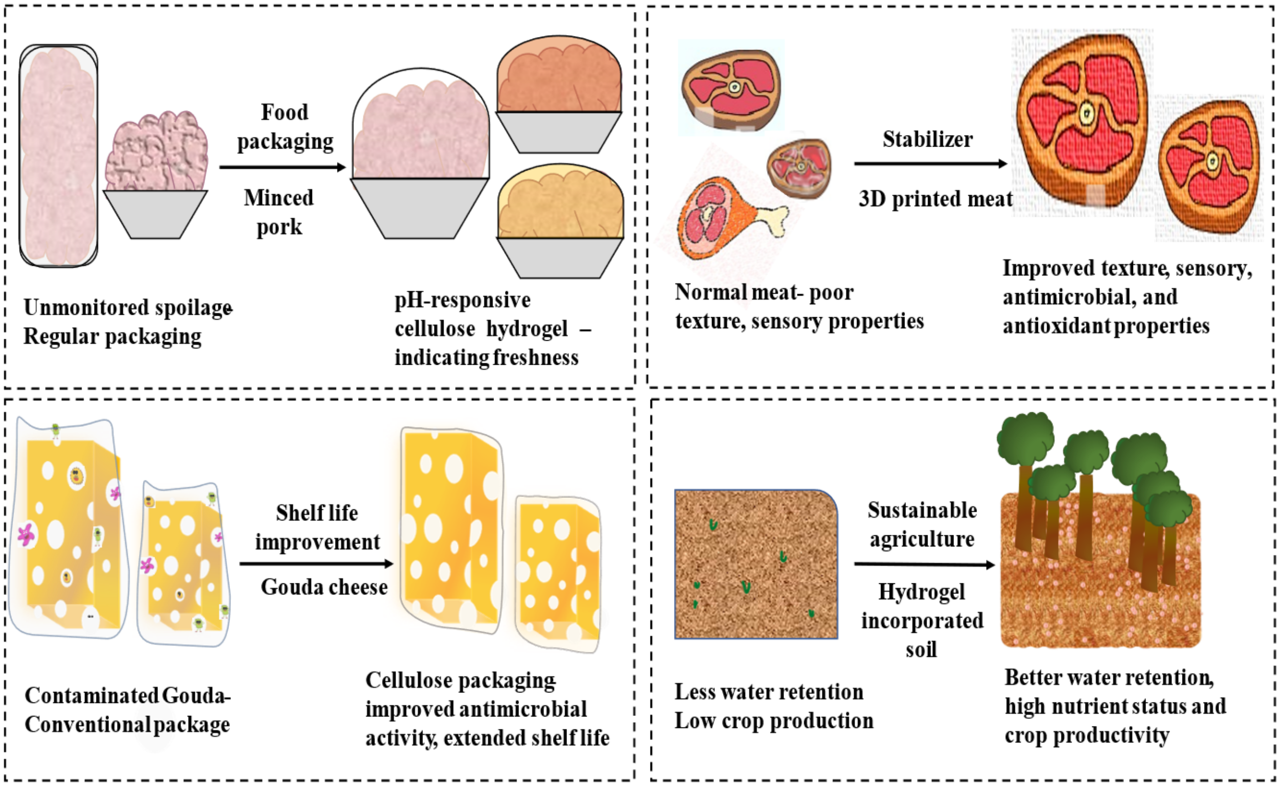

Figure 2.1 Applications of cellulose hydrogels in food-related industries.

2.4.1 Food packaging

The use of nonbiodegradable polymers causes environmental problems such as the accumulation of plastic and persistent organic pollutants that release harmful chemicals into the environment. Food packaging using cellulose hydrogels is an innovative solution to the increasingly serious issue of abundant use and misuse of petroleum-based polymeric materials. In addition, they have been used as hydrogel matrices to incorporate functional fillers to fabricate smart or antimicrobial food packaging and prevent the contamination of food products. For instance, Sutthasupa et al. developed a pH-sensitive colorimetric indicator using the alginate-methylcellulose hydrogel with Ca^{2+} as the crosslinking agent for monitoring the freshness of minced pork [47]. The swelling index of the hydrogel was directly proportional to the percentage of methylcellulose. During the spoilage of meat, the color of the indicator changed from orange to yellow, and there was a positive correlation between the color change and total volatile basic nitrogen produced. Bandyopadhyay et al. constructed bacterial cellulose and guar gum-based polyvinyl pyrrolidone–CMC hydrogel film as an alternative food packaging material for improving the shelf life of packed fruits [48]. Guar gum was incorporated into hydrogel film to increase its mechanical properties. A bagasse cellulose nanofibrils hydrogel-based CO_2-sensitive colorimetric indicator was developed for monitoring fruit spoilage [49]. The carboxylate groups of these 2,2,6,6-tetramethylpiperidine-1-oxyl radical oxidized cellulose nanofibers (TOCNFs) offered high binding affinity to Zn^+ and for the colorimetric indication. Bromothymol blue (0.04 wt%) and methyl red (0.04 wt%) were used as dyes, and the strength of the hydrogel depended on the concentration of TOCNFs. A simple eco-friendly colorimetric freshness indicator was developed for monitoring the freshness of pork samples, which is based on TOCNFs hydrogels with Al^{3+} as crosslinker and anthocyanins for the detection of NH_3 gas [50]. This hydrogel detected the freshness of pork from medium to high warning based on the pH levels of sample both qualitatively and quantitatively and featured the development of a 2nd generation low carbon footprint indicator that could distinguish between various ammonia types. Rao et al. proposed a simple strategy to design multifunctional bilayer bioactive hydrogel membranes by combining CMC complexes containing active microspheres onto a carboxymethyl chitosan gel matrix to enable mechanical stability, good gas barrier properties, good antioxidant and antimicrobial properties, sustained release of active ingredients, and pH responsiveness to epigallocatechin gallate [51]. This multifunctional gel film provided a novel insight into eco-friendly food packaging with the option to alter the functional characteristics. The antimicrobial cellulose hydrogel was mainly based on the incorporation of metallic nanoparticles. For instance, a CMC/gelatin/ZnO nanocomposite hydrogel film was used to reduce photooxidation, authenticate food safety, and increase the shelf life of packaged goods [13]. Firstly, ZnO nanoparticles were incorporated into the CMC and gelatin film-forming solution by solution casting followed by sonication. The 2.5% ZnO-incorporated composite showed the best thermal stability, mechanical properties, and strong antibacterial activity against foodborne pathogenic bacteria, *E. coli*, and *L. monocytogenes*. Gu et al. produced a composite of hyperbranched polyamide-amine/silver nanoparticles and then grafted onto oxidized cellulose to form an antimicrobial cellulose hydrogel film [52]. As shown in Figure 2(a), the incorporation of Ag nanoparticles significantly inhibited the growth of *E. coli* and *S. aureus*, prolonging the shelf life of wrapped cherry tomatoes for 9 days.

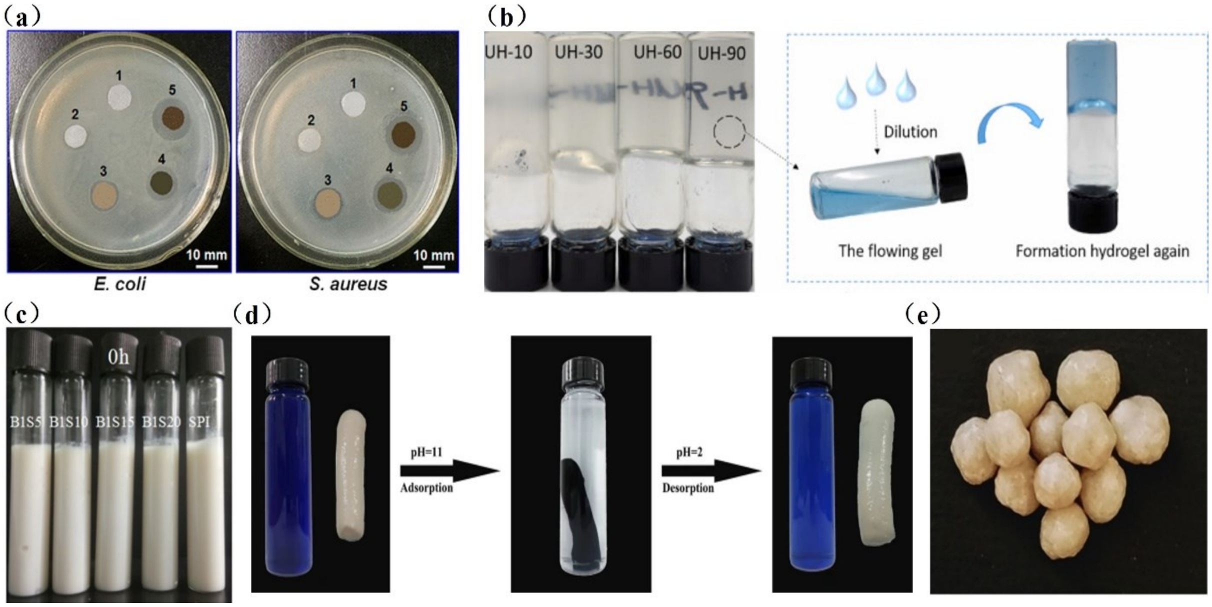

Figure 2.2 Applications of cellulose-based hydrogels for (a) microbial inhibition, [52] (b) stabilization of Pickering emulsions, [53] (c) fat substitution, [54] (d) dye adsorption, [55] and (e) controlled release of fertilizers. [56]

2.4.2 Food additive

The incorporation of food additives promotes nutrient balance, extends the shelf life of food products, and ensures consumer safety. Cellulose hydrogels can be used as emulsifiers, stabilizers, gelling agents, and thickeners. In the research performed by Shahbazi et al., the possibility of developing functional food with personalized preference by 3D printing the food hydrogels with bioactive compounds using multifunctional biopolymeric ink has been explored [57]. The improvement of emulsion stability and bioactivity was investigated using the Pickering emulsion hydrogel, which is composed of microcrystalline cellulose conjugated with 3 different types of polyphenols such as gallic acid, tannic acid, and cyanidin-3-*O*-glucoside by the free-radical grafting method. The developed emulsion gels displayed great mechanical strength, superior 3D-printing ability, improved structural stability and lubrication, superlative thixotropic properties, enhanced matrix chewability, and antioxidant properties. Among the 3 polyphenols, cyanidin-3-*O*-glucoside was determined to potentially enhance the emulsion stability against coalescence and decrease the droplet size of the emulsion gel. A 3D-printed meat mimic with more desirable sensory properties was fabricated based on soy-based emulsions with surface-active microcrystalline cellulose conjugated with gallic acid and lauric arginine, which improved the interfacial stability through intra- and intermolecular hydrogen bonding and hydrophobic interactions [58]. This micro-biosurfactant-emulsion gel produced a multifunctional ink that offered good geometrical characteristics and shape fidelity, viscoelastic behavior, and enhanced juiciness of the meat analogue and fibrousness with improved antimicrobial and antioxidant effects, offering a potential food-grade 3D printed meat analogue. A thermo-gellable polysaccharide curdlan and regenerated cellulose-based emulsion gel was fabricated by Jiang et al [59]. The formulated hydrogel showed enhanced storage modulus and loss modulus, shear thinning behavior, and decreased creep compliance under micro-stress. High internal phase Pickering emulsions stabilized with various concentrations of CNC were a possible solution to improve the compatibility of different materials for printing fidelity, structure, and resolution strength [60]. It was also worth noting that this hydrogel displayed good rheological properties, high solid viscoelasticity, and processability. The 3D object produced from the hydrogel with 0.5 wt% CNC and 50 mM sodium chloride had the best resolution and shape, which was food-grade and had the potential application in edible-emulsion manufacturing sectors. The polyacrylamide organic hydrogels were subjected to Pickering emulsion template polymerization and the resultant porous hydrogels were coated with a combination of Pickering emulsifier (e.g., bromoacetic acid), modified amphoteric hydroxyethyl cellulose grafted with 1-bromododecane, and graphene oxide to develop functionalized pH-sensitive porous hydrogels [61]. The optimal ratio of this hybrid was determined to be 1:1, producing stable emulsion in both the acidic and alkaline environment with decreased negative effects of the electrolyte.

2.4.3 Functional Foods

Functional foods comprise a variety of healthy compounds such as unsaturated fatty acids, probiotics, and bioactive compounds. Cellulose hydrogel can be used in functional foods to transport and deliver nutrients and bioactive substances to alleviate various diseases. Sultana et al. demonstrated that the calcium alginate-CMC beads had significant effects in preserving and delivering tocotrienol-enriched flaxseed oil [62]. Tocotrienol is a beneficial bioactive compound derived from vitamin E, a potent antioxidant and antitumor compound with neuroprotective properties. Flaxseed oil beads added with tocotrienol were chosen for their excellent stability, narrow particle size distribution, and tiny droplet mean diameter. The composite hydrogel prevented oxidation of tocotrienol-rich flaxseed oil during storage at 4 and 65 °C, improving the oxidative stability of the enriched oil. In addition, the loaded beads had better texture, smoother morphology, enhanced thermal stability, and improved gastric tolerance, in comparison with the unloaded oil. Another research disclosed the release of curcumin from a sustainable nanocomposite hydrogel produced from sugarcane bagasse and incorporated with zinc oxide nanoparticles [63]. The incorporation of ZnO enhanced the mechanical and swelling properties and the drug loading and controlled release of curcumin. The cytotoxicity studies revealed that the fabricated hydrogel exhibited anti-cancerous properties and antimicrobial activity against *Staphylococcus aureus* and *Trichophyton Rubrum.* The cellulose extracted from okara exhibited great biodegradability, tensile strength, and zero cytotoxicity [64]. It was stated that the fermentation process enhanced the nutrient content of the okara drastically, and this cellulose hydrogel could also be employed in nutrient delivery. In another study, pineapple pulp cellulose hydrogel was studied for its potential in the controlled delivery of probiotics [65]. The hydrogel was developed by using acrylic acid as the crosslinker in combination with the pineapple pulp cellulose. The fabricated cellulose hydrogel displayed pH-sensitivity and sustained release behavior when incorporated with the probiotics in simulated gastric fluid and simulated intestinal fluid with release rates of 25.05% and 87.02%, respectively. Yan et al. revealed the controlled release of short-chain fatty acids by using celery cellulose hydrogels as the delivery vector [66]. The hydrogel loaded with short-chain fatty acids achieved a maximum loading capacity of around 80%, and the controlled release was easily triggered by using the ultrasound. Thus, the developed hydrogel with high biocompatibility could be used as a promising oral delivery system for functional molecules with the capacity to tune the dosage levels. Guo et al. synthesized a bacterial cellulose/soy protein isolate hydrogel as a fat substitute in ice cream [54]. As shown in Figure 2(c), the incorporation of a low dose of bacterial cellulose (1:20) into soy protein isolate contributed to the hydrogel with improved thermal stability, textural, rheological, and emulsifying properties. The resultant ice cream had low calories, melting resistance, and good textural properties.

2.4.4 Water treatment and purification

The treatment of industrial wastewater is particularly important due to the shortage of water resources and the increasing expansion of industrial units. Cellulose hydrogels have been reported to adsorb both cationic and anionic dyes from wastewater, leading to an efficient and convenient water treatment process. For instance, Wang et al. fabricated a porous CMC/chitosan hydrogel crosslinked by ECH as shown in Figure 2(d) [55]. The swelling ratio of hydrogel under different pH levels was modulated by different compositions. The swelling of hydrogels under acidic condition was largely affected by chitosan content, due to the higher affinity of $-NH_3^+$ to water molecules. However, the swelling under neutral and alkaline conditions was regulated by the CMC content, which was attributed to an increase in the ionized $-COO^-$ content and an increase in the repulsive forces between the molecular chains. Besides, the hydrogel showed the adsorption capacity of 120 mg/g and 95% desorption for methylene blue and the adsorption capacity of 100 mg/g and 90% desorption for acid orange II after five cycles. A similar CMC/chitosan-based hydrogel crosslinked by graphene oxide was reported by Mittal et al., which could adsorb 99% methylene blue at pH 7 and 82% methyl orange at pH 3, corresponding to maximum adsorption capacities of 655.98 and 404.52 mg/g, respectively [67]. Kamel et al. constructed a CMC-grafted acrylamide hydrogel embedded with modified magnetite nanoparticles and porous carbon, which showed maximum adsorption capacity of 294.1 and 222.2 mg/g lead ions and methylene blue, respectively [68]. Dai et al. emphasized the effect of temperature on the adsorption capacity of CMC/PVA hydrogel for the treatment of methylene blue-contained wastewater [69]. The optimum adsorption temperature was 40 °C for the capacity of 157.50 mg/g, while the higher temperature caused higher mobility of the dye molecules, leading to a decrease in the adsorption effect. Malatji et al. fabricated a reusable magnetic hydrogel nanocomposite composed of CMC, polyacrylic acid, and clay, which could adsorb about 98% methylene blue after four cycles of adsorption-desorption [70]. Huang et al. proposed an ECH crosslinked hydroxyethyl cellulose/PVA hydrogel for dye removal [71]. The obtained hydrogels possessed a swelling rate of up to 1,220 g/g and could adsorb large amounts of the positively charged dyes (rhodamine 6G, crystal violet, and methylene blue) at 153, 184, and 196 mg/g, respectively. Ao et al. fabricated a citric acid crosslinked hydrogel membrane by dip-coating filter paper in a cellulose solution, which could adsorb 73% methylene blue at 100 ppm and 95% oil/water separation efficiency after three cycles [72].

2.4.5 Sustainable agriculture

Sustainable agriculture relies on the effective management of fertilizers and plays an important role in reducing environmental threats. Cellulose hydrogels can be used in sustainable agriculture to control the release of nutrients from fertilizers into the soil environment to combat nutrient leaching, enable efficient utilization of water resources, and address the growing global demand for food without the concern of environmental pollution caused by non-biodegradable materials. Rizwan et al. synthesized a composite hydrogel based on *Acer platanoides* cellulose using methylene bisacrylamide as a crosslinker [73]. Urea and calcium superphosphate as two nutrients were sprayed with an epoxy solution in acetone, followed by two coating processes of hydrogel to form a composite. The resultant hydrogel showed a swelling ratio of 88.8% in de-ionized water and a controlled release behavior described by the Korsmeyer-Peppas model, leading to 80% release of the nitrogen content and 72% of the phosphorus within 60 days. Akalin and Pulat compared CMC hydrogel crosslinked by iron (III) chloride hexahydrate and carrageenan hydrogel crosslinked by glutaraldehyde. CMC hydrogel had better water retention capacity and could increase the water content in the soil from 13% to 76% on the 10th day [74]. Besides, the longer release time (30 hours) of loaded zinc-nanoparticles was also found in CMC hydrogel, which significantly stimulated the growth of wheatgrass. A biodegradable hydrogel from acid whey and CMC crosslinked by citric acid was produced by Čechmánková et al [75]. The incorporation of hydrogel increased the water holding capacity by up to 15% without adverse side effects on soil properties. Furthermore, the availability of phosphorus and potassium levels was increased to 50 and 84%, which was beneficial for crop growth. Shaghaleh et al. fabricated a pH-responsive and sustained released nitrogen fertilizer hydrogel based on aminated cellulose nanofiber and cationic copolymer [76]. Ionic interactions and hydrogen bonding reduced the pore size of the network structure and improved sustained-release properties. The produced hydrogel showed the lowest release rate in the neutral media while the highest release rate in the acidic condition, which was related to the swelling of hydrogel. Sustained releases of ammonium nitrate from hydrogel at pH 5.5 and 7.4 were 2.69 mg/day and 0.55 mg/day, respectively, leading to a positive impact on rice growth. A slow-release fertilizer hydrogel based on hydroxyl propyl methyl cellulose, PVA, glycerol, and blended paper was reported by Kareem et al [77]. The swelling ratio of hydrogel was 15.2 g/g in tap water, which delayed the release of urea in soil from 97% to 87.01% within 4 days. Besides, the diffusion process could be described by the first-order kinetic model, which was regulated by the concentration of urea and the diffusion pathway of the hydrogel structure.

2.5 CONCLUSIONS AND OUTLOOK

The development of cellulose-based hydrogels for food-related applications has become prominent due to many desirable properties of cellulose such as biodegradability, eco-friendliness, and availability. The network structure and physicochemical properties of cellulose hydrogels can be easily manipulated. Cellulose-based hydrogels have been applied in various areas, such as intelligent and antibacterial food packaging, emulsion stabilizers, functional foods, wastewater treatment, sustained agriculture, etc. However, future research on cellulose-based hydrogels may be required in the following areas:

1. The application of chemical crosslinkers can lead to the denser network and stable structure of cellulose hydrogels. However, the amount of crosslinker residue and their impact on the biodegradation of cellulose hydrogels should be evaluated.

2. The feasibility of cellulose-based hydrogels in food-related applications should be evaluated. Processes for mass production should be available and the cross-linking of the hydrogels should be economically practical. The selection of cost-effective materials to produce hydrogel and a simplified production process will help to reduce the cost of cellulose-based hydrogels.

2.6 REFERENCES

1. Wichterle, O., & Lim, D. (1960). Hydrophilic gels for biological use. *Nature*, *185*(4706), 117-118.

2. Behera, S., & Mahanwar, P. A. (2020). Superabsorbent polymers in agriculture and other applications: a review. *Polymer-Plastics Technology and Materials*, *59*(4), 341-356.

3. Aswathy, S. H., Narendrakumar, U., & Manjubala, I. (2020). Commercial hydrogels for biomedical applications. *Heliyon*, *6*(4), E03719.

4. Nie, J., Pei, B., Wang, Z., & Hu, Q. (2019). Construction of ordered structure in polysaccharide hydrogel: A review. *Carbohydrate polymers*, *205*, 225-235.

5. Nasution, H., Harahap, H., Dalimunthe, N. F., Ginting, M. H. S., Jaafar, M., Tan, O. O., ... & Herfananda, A. L. (2022). Hydrogel and effects of crosslinking agent on cellulose-based hydrogels: A review. *Gels*, *8*(9), 568.

6. Huang, K., & Wang, Y. (2022). Recent applications of regenerated cellulose films and hydrogels in food packaging. *Current Opinion in Food Science*, *43*, 7-17.

7. Kabir, S. F., Sikdar, P. P., Haque, B., Bhuiyan, M. R., Ali, A., & Islam, M. N. (2018). Cellulose-based hydrogel materials: Chemistry, properties and their prospective applications. *Progress in biomaterials*, *7*, 153-174.

8. Bustamante-Torres, M., Romero-Fierro, D., Arcentales-Vera, B., Palomino, K., Magaña, H., & Bucio, E. (2021). Hydrogels classification according to the physical or chemical interactions and as stimuli-sensitive materials. *Gels*, *7*(4), 182.

9. Zainal, S. H., Mohd, N. H., Suhaili, N., Anuar, F. H., Lazim, A. M., & Othaman, R. (2021). Preparation of cellulose-based hydrogel: A review. *Journal of Materials Research and Technology*, *10*, 935-952.

10. Kundu, R., Mahada, P., Chhirang, B., & Das, B. (2022). Cellulose hydrogels: Green and sustainable soft biomaterials. *Current Research in Green and Sustainable Chemistry*, *5*, 100252.

11. Chang, C., & Zhang, L. (2011). Cellulose-based hydrogels: Present status and application prospects. *Carbohydrate polymers*, *84*(1), 40-53.

12. Thivya, P., Akalya, S., & Sinija, V. R. (2022). A comprehensive review on cellulose-based hydrogel and its potential application in the food industry. *Applied Food Research*, *2*(2), 100161.

13. Zafar, A., Khosa, M. K., Noor, A., Qayyum, S., & Saif, M. J. (2022). Carboxymethyl cellulose/gelatin hydrogel films loaded with zinc oxide nanoparticles for sustainable food packaging applications. *Polymers*, *14*(23), 5201.

14. Zhao, Y., Zhou, S., Xia, X., Tan, M., Lv, Y., Cheng, Y., ... & Wang, H. (2022). High-performance carboxymethyl cellulose-based hydrogel film for food packaging and preservation system. *International Journal of Biological Macromolecules*, *223*, 1126-1137.

15. Hu, Y., Hu, S., Zhang, S., Dong, S., Hu, J., Kang, L., & Yang, X. (2021). A double-layer hydrogel based on alginate-carboxymethyl cellulose and synthetic polymer as sustained drug delivery system. *Scientific reports*, *11*(1), 9142.

16. Moharrami, P., & Motamedi, E. (2020). Application of cellulose nanocrystals prepared from agricultural wastes for synthesis of starch-based hydrogel nanocomposites: Efficient and selective nanoadsorbent for removal of cationic dyes from water. *Bioresource technology*, *313*, 123661.

17. Santoso, S. P., Kurniawan, A., Soetaredjo, F. E., Cheng, K. C., Putro, J. N., Ismadji, S., & Ju, Y. H. (2019). Eco-friendly cellulose–bentonite porous composite hydrogels for adsorptive removal of azo dye and soilless culture. *Cellulose*, *26*, 3339-3358.

18. Godiya, C. B., Cheng, X., Li, D., Chen, Z., & Lu, X. (2019). Carboxymethyl cellulose/polyacrylamide composite hydrogel for cascaded treatment/reuse of heavy metal ions in wastewater. *Journal of hazardous materials*, *364*, 28-38.

19. Bauli, C. R., Lima, G. F., de Souza, A. G., Ferreira, R. R., & Rosa, D. S. (2021). Eco-friendly carboxymethyl cellulose hydrogels filled with nanocellulose or nanoclays for agriculture applications as soil conditioning and nutrient carrier and their impact on cucumber growing. *Colloids and Surfaces A: Physicochemical and Engineering Aspects*, *623*, 126771.

20. He, A., Li, S., Ma, J., & Yang, Z. (2014). Environmental friendly polymer materials for sustainable development. *International Journal of Polymer Science*, *2014*(1), 107028.

21. Palantöken, S., Bethke, K., Zivanovic, V., Kalinka, G., Kneipp, J., & Rademann, K. (2020). Cellulose hydrogels physically crosslinked by glycine: Synthesis, characterization, thermal and mechanical properties. *Journal of Applied Polymer Science, 137*(7), 48380.

22. Mali, K., Dhawale, S., Dias, R., Dhane, N., & Ghorpade, V. (2018). Citric acid crosslinked carboxymethyl cellulose-based composite hydrogel films for drug delivery. *Indian Journal of Pharmaceutical Sciences, 80*(4), 657-667.

23. Tavera-Quiroz, M. J., Díaz, J. J. F., & Pinotti, A. (2018). Characterization of methylcellulose based hydrogels by using citric acid as a crosslinking agent. *International Journal of Applied Engineering Research, 13*(17), 13302-13307.

24. Pavandi, N., Taghavi, E., & Anarjan, N. (2021). Preparation of carboxymethyl cellulose and polyvinyl alcohol (CMC/PVA) hydrogels using freeze−thaw processes for adsorption of Zn2+ and Cu2. *Cellulose Chemistry and Technology, 55*(3-4), 375-383.

25. Li, Z., Yu, R., & Guo, B. (2021). Shape-memory and self-healing polymers based on dynamic covalent bonds and dynamic noncovalent interactions: Synthesis, mechanism, and application. *ACS Applied Bio Materials, 4*(8), 5926-5943.

26. Sekine, Y., Nankawa, T., Yunoki, S., Sugita, T., Nakagawa, H., & Yamada, T. (2020). Eco-friendly carboxymethyl cellulose nanofiber hydrogels prepared via freeze cross-linking and their applications. *ACS Applied Polymer Materials, 2*(12), 5482-5491.

27. Liu, X., Yang, K., Chang, M., Wang, X., & Ren, J. (2020). Fabrication of cellulose nanocrystal reinforced nanocomposite hydrogel with self-healing properties. *Carbohydrate Polymers, 240*, 116289.

28. Hu, D., Zeng, M., Sun, Y., Yuan, J., & Wei, Y. (2021). Cellulose-based hydrogels regulated by supramolecular chemistry. *SusMat, 1*(2), 266-284.

29. Tuan Mohamood, N. F. A.-Z., Abdul Halim, A. H., & Zainuddin, N. (2021). Carboxymethyl cellulose hydrogel from biomass waste of oil palm empty fruit bunch using calcium chloride as crosslinking agent. *Polymers, 13*(23), 4056.

30. Li, D., Liu, N., Yao, X., et al. (2023). Characterization of semi-interpenetrating hydrogel based on Artemisia sphaerocephala Krasch Polysaccharide and cellulose nanocrystals crosslinked by ferric ions. *Food Hydrocolloids, 130*, 108596.

31. Priyadarshi, R., Kumar, B., & Rhim, J.-W. (2020). Green and facile synthesis of carboxymethylcellulose/ZnO nanocomposite hydrogels crosslinked with Zn2+ ions. *International Journal of Biological Macromolecules, 162*, 229-235.

32. Caló, E., & Khutoryanskiy, V. V. (2015). Biomedical applications of hydrogels: A review of patents and commercial products. *European Polymer Journal, 65*, 252-267.

33. Uliniuc, A., Hamaide, T., Popa, M., & Băcăiță, S. (2013). Modified starch-based hydrogels cross-linked with citric acid and their use as drug delivery systems for levofloxacin. *Soft Materials, 11*(4), 483-493.

34. Parhi, R. (2017). Cross-linked hydrogel for pharmaceutical applications: A review. *Advanced Pharmaceutical Bulletin, 7*(4), 515-530.

35. Nuruddin, M., Korani, D. M., Jo, H., et al. (2020). Gas and water vapor barrier performance of cellulose nanocrystal–citric acid-coated polypropylene for flexible packaging. *ACS Applied Polymer Materials, 2*(11), 4405-4414.

36. Wen, L., Liang, Y., Lin, Z., et al. (2021). Design of multifunctional food packaging films based on carboxymethyl chitosan/polyvinyl alcohol crosslinked network by using citric acid as a crosslinker. *Polymer, 230*, 124048.

37. Nguyen, H. T., Ngwabebhoh, F. A., Saha, N., Saha, T., & Saha, P. (2022). Gellan gum/bacterial cellulose hydrogel crosslinked with citric acid as an eco-friendly green adsorbent for safranin and crystal violet dye removal. *International Journal of Biological Macromolecules, 222*, 77-89.

38. Kanafi, N. M., Rahman, N. A., & Rosdi, N. H. (2019). Citric acid cross-linking of highly porous carboxymethyl cellulose/poly (ethylene oxide) composite hydrogel films for controlled release applications. *Materials Today: Proceedings, 7*, 721-731.

39. Lungu, A., Cernencu, A. I., Dinescu, S., et al. (2021). Nanocellulose-enriched hydrocolloid-based hydrogels designed using a Ca2+ free strategy based on citric acid. *Materials & Design, 197*, 109200.

40. Udoetok, I. A., Dimmick, R. M., Wilson, L. D., & Headley, J. V. (2016). Adsorption properties of cross-linked cellulose-epichlorohydrin polymers in aqueous solution. *Carbohydrate Polymers, 136*, 329-340.

41. Han, C., Cao, M., Yu, J., et al. (2023). Carboxymethyl cellulose-based composite polymer hydrogels cross-linked with epichlorohydrin and application for Cu(II) removal. *ACS Applied Polymer Materials, 5(3),* 2070–2078.

42. Chen, X., Chen, C., & Zhu, J. (2019). Facile preparation of cellulose–attapulgite nanocomposite hydrogel for dye adsorption. *Iranian Polymer Journal, 28*, 347-359.

43. Nguyen, M. N., Tran, T. T., Nguyen, Q. T., Tran Thi, T., Nguyen, B. C., & Hollmann, D. (2022). Simple synthesis of cellulose hydrogels based on the direct dissolution of cellulose in tetrabutylphosphonium hydroxide followed by crosslinking. *Polymer Advanced Technologies, 33*(10), 3376-3385.

44. Jeon, J. G., Kim, H. C., Palem, R. R., Kim, J., & Kang, T. J. (2019). Cross-linking of cellulose nanofiber films with glutaraldehyde for improved mechanical properties. *Materials Letters, 250*, 99-102.

45. Rana, J., Goindi, G., & Kaur, N. (2022). Potential prospects of cellulose acetate/acrylic acid-glutaraldehyde semi-interpenetrating networks to remove methylene blue dye from wastewater. *Materials Today: Proceedings, 68*, 996-1002.

46. Wahid, F., Hu, X-H., Chu, L-Q., Jia, S-R., Xie, Y-Y., & Zhong, C. (2019). Development of bacterial cellulose/chitosan based semi-interpenetrating hydrogels with improved mechanical and antibacterial properties. *International Journal of Biological Macromolecules, 122*, 380-387.

47. Sutthasupa, S., Padungkit, C., & Suriyong, S. (2021). Colorimetric ammonia (NH3) sensor based on an alginate-methylcellulose blend hydrogel and the potential opportunity for the development of a minced pork spoilage indicator. *Food Chemistry, 362*, 130151.

48. Bandyopadhyay, S., Saha, N., Brodnjak, U. V., & Sáha, P. (2019). Bacterial cellulose and guar gum based modified PVP-CMC hydrogel films: Characterized for packaging fresh berries. *Food Packaging and Shelf Life, 22*, 100402.

49. Lu, P., Liu, R., Liu, X., & Wu, M. (2018). Preparation of self-supporting bagasse cellulose nanofibrils hydrogels induced by zinc ions. *Nanomaterials, 8*(10), 800.

50. Pirayesh, H., Park, B-D., Khanjanzadeh, H., Park, H-J., & Cho, Y-J. (2023). Nanocellulose-based ammonia sensitive smart colorimetric hydrogels integrated with anthocyanins to monitor pork freshness. *Food Control, 147*, 109595.

51. Rao, Z., Lei, X., Chen, Y., Ling, J., Zhao, J., & Ming, J. (2023). Facile fabrication of robust bilayer film loaded with chitosan active microspheres for potential multifunctional food packing. *International Journal of Biological Macromolecules, 231,* 123362.

52. Gu, R., Yun, H., Chen, L., Wang, Q., & Huang, X. (2019). Regenerated cellulose films with amino-terminated hyperbranched polyamic anchored nanosilver for active food packaging. *ACS Applied Bio Materials, 3*(1), 602-610.

53. Ni, Y., Wu, J., Jiang, Y., Li, J., Fan, L., & Huang, S. (2022). High-internal-phase Pickering emulsions stabilized by ultrasound-induced nanocellulose hydrogels. *Food Hydrocolloids, 125*, 107395.

54. Guo, Y., Zhang, X., Hao, W., et al. (2018). Nano-bacterial cellulose/soy protein isolate complex gel as fat substitutes in ice cream model. *Carbohydrate Polymers, 198*, 620-630.

55. Wang, W., Hu, J., Zhang, R., Yan, C., Cui, L., & Zhu, J. (2021). A pH-responsive carboxymethyl cellulose/chitosan hydrogel for adsorption and desorption of anionic and cationic dyes. *Cellulose, 28*, 897-909.

56. Kassem, I., Ablouh, E-H., El Bouchtaoui, F-Z., et al. (2022). Biodegradable all-cellulose composite hydrogel as eco-friendly and efficient coating material for slow-release MAP fertilizer. *Progress in Organic Coatings, 162*, 106575.

57. Shahbazi, M., Jäger, H., & Ettelaie, R. (2021). Development of an antioxidative Pickering emulsion gel through polyphenol-inspired free-radical grafting of microcrystalline cellulose for 3D food printing. *Biomacromolecules, 22*(11), 4592-4605.

58. Shahbazi, M., Jäger, H., & Ettelaie, R. (2022). A Promising Therapeutic Soy-Based Pickering Emulsion Gel Stabilized by a Multifunctional Microcrystalline Cellulose: Application in 3D Food Printing. *Journal of Agricultural and Food Chemistry, 70*(7), 2374-2388.

59. Jiang, Y., Liu, L., Wang, B., et al. (2019). Polysaccharide-based edible emulsion gel stabilized by regenerated cellulose. *Food Hydrocolloids, 91*, 232-237.

60. Ma, T., Cui, R., Lu, S., et al. (2022). High internal phase Pickering emulsions stabilized by cellulose nanocrystals for 3D printing. *Food Hydrocolloids, 125*, 107418.

61. Wang, X., He, J., Ma, L., Yan, B., Shi, L., & Ran, R. (2021). Self-assembling graphene oxide/modified amphipathic hydroxyethyl cellulose hybrid stabilized Pickering emulsion polymerization for functional hydrogel. *Colloids and Surfaces A: Physicochemical and Engineering Aspects, 610*, 125742.

62. Sultana, M., Chan, E. S., Janarthanan, P., & Choo, W. S. (2023). Encapsulation of Tocotrienol-Enriched Flaxseed Oil in Calcium Alginate–Carboxymethyl Cellulose

Hydrogel Beads for Improved Oxidative Stability and Release Profile. *ACS Food Science & Technology, 3(2),* 259-272.

63. George, D., Maheswari, P. U., Sheriffa Begum, K. M. M., & Arthanareeswaran, G. (2019). Biomass-derived dialdehyde cellulose cross-linked chitosan-based nanocomposite hydrogel with phytosynthesized zinc oxide nanoparticles for enhanced curcumin delivery and bioactivity. *Journal of Agricultural and Food Chemistry, 67*(39), 10880-10890.

64. Cui, X., Lee, J. J., & Chen, W. N. (2019). Eco-friendly and biodegradable cellulose hydrogels produced from low cost okara: towards non-toxic flexible electronics. *Scientific Reports, 9*(1), 1-9.

65. Xing, Y., & Huang, H. (2021). Preparation of pineapple pulp cellulose hydrogel and its adsorption and release characteristics toward probiotics. *Food Science, 42*, 8-14.

66. Ai, B., Zheng, L., Li, W., et al. (2021). Biodegradable cellulose film prepared from banana pseudo-stem using an ionic liquid for mango preservation. *Frontiers in Plant Science, 12*, 234.

67. Mittal, H., Al Alili, A., Morajkar, P. P., & Alhassan, S. M. (2021). GO crosslinked hydrogel nanocomposites of chitosan/carboxymethyl cellulose–A versatile adsorbent for the treatment of dyes contaminated wastewater. *International Journal of Biological Macromolecules, 167*, 1248-1261.

68. Kamel, S., El-Gendy, A. A., Hassan, M. A., El-Sakhawy, M., & Kelnar, I. (2020). Carboxymethyl cellulose-hydrogel embedded with modified magnetite nanoparticles and porous carbon: Effective environmental adsorbent. *Carbohydrate Polymers, 242*, 116402.

69. Dai, H., Huang, Y., & Huang, H. (2018). Eco-friendly polyvinyl alcohol/carboxymethyl cellulose hydrogels reinforced with graphene oxide and bentonite for enhanced adsorption of methylene blue. *Carbohydrate Polymers, 185*, 1-11.

70. Malatji, N., Makhado, E., Ramohlola, K. E., et al. (2020). Synthesis and characterization of magnetic clay-based carboxymethyl cellulose-acrylic acid hydrogel nanocomposite for methylene blue dye removal from aqueous solution. *Environmental Science and Pollution Research, 27*, 44089-44105.

71. Huang, S., Wu, L., Li, T., Xu, D., Lin, X., & Wu, C. (2019). Facile preparation of biomass lignin-based hydroxyethyl cellulose super-absorbent hydrogel for dye pollutant removal. *International Journal of Biological Macromolecules, 137*, 939-947.

72. Ao, C., Zhao, J., Li, Q., et al. (2020). Biodegradable all-cellulose composite membranes for simultaneous oil/water separation and dye removal from water. *Carbohydrate Polymers, 250*, 116872.

73. Rizwan, M., Gilani, S. R., Durrani, A. I., & Naseem, S. (2022). Kinetic model studies of controlled nutrient release and swelling behavior of combo hydrogel using Acer platanoides cellulose. *Journal of the Taiwan Institute of Chemical Engineers, 131*, 104137.

74. Akalin, G. O., & Pulat, M. (2020). Controlled release behavior of zinc-loaded carboxymethyl cellulose and carrageenan hydrogels and their effects on wheatgrass growth. *Journal of Polymer Research, 27*(1), 6.

75. Čechmánková, J., Skála, J., Sedlařík, V., et al. (2021). The synergic effect of whey-based hydrogel amendment on soil water holding capacity and availability of nutrients for more efficient valorization of dairy by-products. *Sustainability, 13*(19), 10701.

76. Shaghaleh, H., Hamoud, Y. A., Xu, X., Wang, S., & Liu, H. (2022). A pH-responsive/sustained release nitrogen fertilizer hydrogel based on aminated cellulose nanofiber/cationic copolymer for application in irrigated neutral soils. *Journal of Cleaner Production, 368*, 133098.

77. Kareem, S. A., Dere, I., Gungula, D. T., et al. (2021). Synthesis and characterization of slow-release fertilizer hydrogel based on hydroxy propyl methyl cellulose, polyvinyl alcohol, glycerol and blended paper. *Gels, 7*(4), 262.

CONNECTING STATEMENT I

Chapter 2 focused on the recent advancements of cellulose-based hydrogels for food-related applications. This review provides an overview of the preparation methods involved in the fabrication of cellulose-based hydrogels and their diverse applications in food industries, wastewater treatment, and agricultural sectors. **Chapter 3** involved developing cotton fabric derived-cellulose hydrogel coolants with a special core-shell structure formed by the dip-coating technique. This study investigated the structural, mechanical, water retention, and thermal properties of the cellulose-based hydrogels and comparative analysis of their cooling and thawing patterns with the conventional ice cubes.

CHAPTER 3. SUSTAINABLE AND ROBUST CELLULOSE-BASED CORE-SHELL HYDROGELS RECYCLED FROM WASTE COTTON FABRICS AS HIGH-PERFORMANCE FOOD COOLANTS

3.1 ABSTRACT

Ideal temperature condition is one of the essential determinants that critically impact the quality of food products. Conventional methods of employing water-based ice cubes present challenges from meltwater being breeding grounds for microorganisms and heightening the risk for cross-contamination. Hereby, the presented cellulose-based hydrogels crosslinked by epichlorohydrin are dip-coated with alginate/calcium chloride to form a core-shell structure for achieving the critical benchmarks of an ideal food coolant with limited meltwater production, high-water retention capacity, and high mechanical strength. The structures and properties of the hydrogels before and after freeze-thaw cycles are characterized by scanning electron microscopy, compressive test, water retention test, and differential scanning calorimetry. All formulated hydrogels demonstrate promising compressive strength, latent heat of fusion, and water retention properties. Notably, the C2A10Cl hydrogel exhibits a maximum compressive strength of 144.7 kPa and high latent heat of fusion of 272.5 J/g, which are better than previously reported sustainable hydrogel coolants. Furthermore, comparison studies reveal that the cellulose-based hydrogels demonstrate a similar thawing pattern to conventional ice cubes but without the generation of any meltwater. The temperature of blueberries can be cooled down from 22 °C to 3.9 °C in 32 minutes by the hydrogels and in 26 minutes by ice cubes, respectively.

Keywords: cellulose hydrogel, food coolant, waste textile, sustainable, core-shell structure

3.2 INTRODUCTION

Temperature is one of the most critical factors that influences the quality and safety of food products. Optimal temperature range plays an inevitable role in slowing down moisture loss and metabolic activities, thereby improving food sustainability and security. [1] Any fluctuations in the temperature led to microbial cross-contamination deteriorate the shelf life of food products, resulting in the global challenges of food wastage and economic loss. Every year, nearly one-third of the produced food ends up as waste. [2] In developing countries, it has been estimated that food wastage during the post-harvest process is about 40%, which is due to technological constraints and deficient storage and handling practices. [3] The microbial spoilage of food products and their consumption have resulted in about 600 million foodborne illness cases and 420,000 deaths annually. [4] To address microbial spoilage-related issues and extend shelf life, water-based cooling systems are widely used in the food industry because of their low cost and high heat-absorption capacity at the phase-transition temperature (near 0 °C). However, the pressing issue of meltwater that can be generated from traditional ice cubes may cause secondary contaminations. Other efficient cooling methods such as refrigerated trucks and containers, insulation boxes, etc., still have cost- and/or energy-related drawbacks. [5,6] Consequently, it can be inferred that there is an evident gap in the development of sustainable and reliable food coolants.

Hydrogels are fabricated by the crosslinking of polymer molecular chains, which endows them with the ability to absorb and withhold a large amount of water within their porous polymeric networks. [7] Physical interactions such as hydrogen bonds, [8] electrostatic interactions, [9] and hydrophobic interactions, [10] and chemical crosslinking enabled by forming covalent bonds between the functional groups of the polymers are the most commonly used strategies. [11-16] Hydrogels have many applications in the food and pharmaceutical industries, specifically in food packaging, hydrogel-based sensors indicating food spoilage, and encapsulation of bioactive compounds for sustained release systems. [17, 18] Cellulose is a biopolymer with linearly arranged glucose units linked by the β-1,4-glycosidic bonds. [19] It is of great research value attributing to its abundance in nature and numerous hydroxyl groups, and it can be utilized for the fabrication of hydrogels with fascinating characteristics such as great mechanical strength, adjustable swelling ability, and possible responsiveness to time, pH, and temperature. [20] Cellulose-based hydrogels are also a promising biomaterial that can contribute to sustainable development. [21]

Cotton is one of the main natural sources of raw materials, and cotton fibers are composed of about 95% cellulose. [22] Nearly 25 million tons of cotton fabrics are produced annually with increasingly higher levels of waste being generated on a global scale. [23] About 95% of post-consumer cotton products are either incinerated or dumped into landfills, leading to the production and release of greenhouse gases. [24] In our previous works, cellulose films and hydrogels have been fabricated from waste cotton fabrics by dissolution and regeneration in ‘green’ aqueous solvent systems. [25, 26] It was worth noting that, Zou et al. and Zheng et al. recently highlighted the potential of hydrogels made by gelatin and corn starch as a promising choice for the development of an ideal food coolant. [27-29] Based on our current understanding, there has been no prior exploration to develop hydrogel-based food coolants from post-consumer waste materials. Herein, waste cotton textiles were used as the raw materials for constructing the cellulose-based coolants with the focus on strategizing the potential recycling of waste cotton fabrics into sustainable products.

It has been previously stated that an ideal coolant system is anticipated to exhibit good mechanical strength to bear the load of food products during transportation, heat absorbing capacity and cooling efficiency through multiple freeze-thaw cycles, water retention with minimal meltwater production, and stability after several freeze-thaw cycles. [27-29] Hence, we hypothesize that the chemically crosslinked cellulose-based hydrogels coated with alginate can act as a strong core-shell matrix for water retention, so as to fulfill the critical characteristics of the envisioned hydrogel-ice cubes. The obtained cellulose-based hydrogels were tested before and after 5 freeze-thaw cycles to investigate the morphology, compressive strength, water retention, and latent heat of fusion. The optimized sample was compared with conventional ice cubes to evaluate the thawing behavior and cooling efficiency.

3.3 RESULTS AND DISCUSSION

3.3.1 Cellulose-based hydrogel morphology

The surface and cross-sectional area of cellulose-based hydrogels were observed by SEM. As shown in **Figure 1**, all the samples had a thin coating layer (marked by the doted lines) and similar porous structures. The large holes in the structure were beneficial to the storage of water, and no obvious changes were observed after 5 cycles of freeze-thaw treatment, suggesting the good stability of chemically crosslinked hydrogel networks. [30] It was worth noting that the addition of 20% alginate in the hydrogel forming solutions did not alter the porous structure. The surface morphology of cellulose-based hydrogels is shown in **Figure 2**. The shell layers were very compact due to the chelation between alginate and $CaCl_2$. [31] Neither the freeze-thaw treatment nor the concentration of $CaCl_2$ in the dip-coating solution affected the intactness and thickness of the shell layers. This thin layer was expected to provide mechanical support; at the same time, it did not affect the overall water content of cellulose-based hydrogels too much. [32]

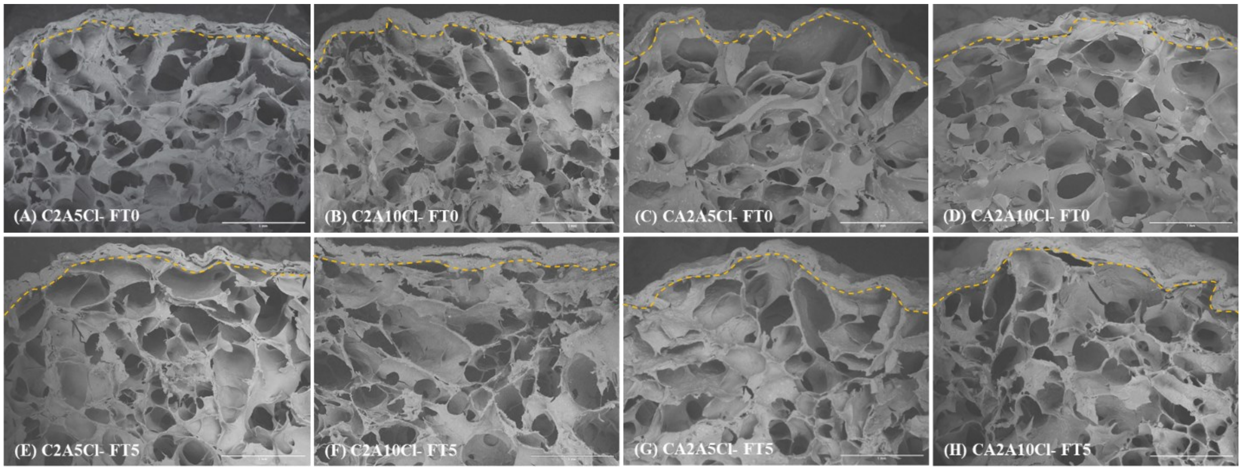

Figure 3.1 SEM images of cross-sections of cellulose-based hydrogels before (upper) and after (below) five cycles of freeze-thaw treatment. *The dotted lines indicate the shell layers. Scale bar: 1 mm.

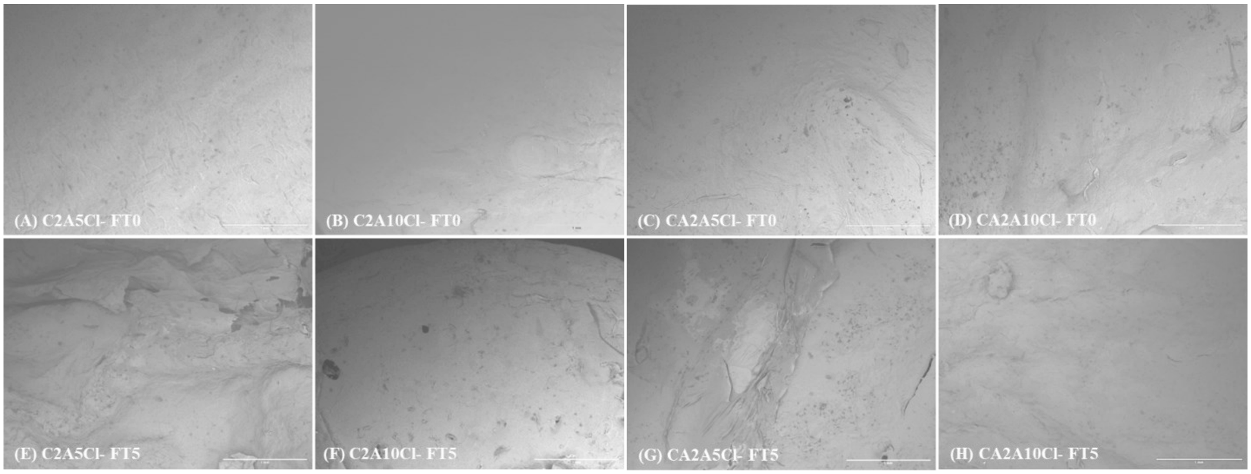

Figure 3.2 SEM images of surface morphology of cellulose-based hydrogels before (upper) and after (below) five cycles of freeze-thaw treatment. Scale bar: 1 mm.

3.3.2 Cellulose-based hydrogel properties

3.3.2.1 Mechanical Properties

The effects of hydrogel matrix composition, Ca^{2+} ion concentration in coating solution, and freeze-thaw cycles on the compressive strength of cellulose-based hydrogels were investigated. As shown in **Figure 3**, the presence of alginate in the matrices resulted in relatively weaker hydrogels. The compressive strength of C2A5Cl was 93.1±7.3 kPa, which reduced to 83.0±2.7 kPa for CA2A5Cl, and C2A10Cl and CA2A10Cl followed the same trend. It was because cellulose acted as the structural framework, effectuating the formation of hydrogels, and the decrease in the compressive strength could be due to the weakening of cellulose networks upon the inclusion of alginate, as demonstrated in a previous study. [33] On the other hand, the increase in Ca^{2+} ion concentration from 5% to 10% generated stronger hydrogels. [34] The C2A10Cl hydrogel exhibited the highest compressive strength of 144.7±5.5 kPa. This increase in the compressive strength of C2A10Cl, in comparison to C2A5Cl, could be attributed to the higher intensified cross-linking effect with more Ca^{2+} ions that supported the polymeric networks. [35]

It was worth noting that a drastic drop in the compressive strength of all the hydrogels occurred after the first freeze-thaw cycle. The hydrogels possessed a compressive strength between 24.0 ±2.0 to 43.3 ± 2.0 kPa, and C2A5Cl, C2A10Cl, and CA2A5Cl even broke before withstanding 60% strain. Similar phenomena have been reported by previous literature, [27, 28, 32, 36] and it could be explained by the development of various large/medium-sized ice grains that disturbed the polymer networks. [37-39] The compressive strength of cellulose-based hydrogels was partially restored after more freeze-thaw cycles. The C2A10Cl hydrogel possessed a compressive strength of 87.1±1.7 kPa after 5 freeze-thaw cycles and displayed a good shape recovery to its original height after the compression. This could be due to the physical crosslinking phenomenon that increased the density and stiffness of the hydrogels. [40] During the freezing step, the rearrangement of polymer chains enhanced the physical crosslinking by increasing the number of hydrogen bonds and higher establishments of ionic bonds between Ca^{2+} ions and negatively charged polymers. [41] Once the thawing process was completed, the newly formed interactions remained and integrated with the pre-existing networks, giving additional elasticity and stability to the hydrogels as the number of freeze-thaw cycles increased. [42,43]

Compared to other previously reported hydrogel coolants, the mechanical performance of the cellulose-based hydrogels was remarkable. For instance, the compressive strength of gelatin hydrogels showed a significant drop from 67.9 kPa to 11.03 kPa after one freeze-thaw cycle and remained between 10-16 kPa after 5 freeze-thaw cycles. [28] A drastic drop of the compressive strength from 143.3 kPa to 12.7 kPa was observed in the gelatin/menadione sodium bisulfite hydrogels, which remained low in the consecutive cycles. [32] Similarly, the gelatin/menadione sodium bisulfite hydrogels and photo-crosslinked ones showed compressive strengths of 41.3 kPa and 91.93 kPa before freeze-thaw treatments and reduced to 29.3 kPa and 69.9 kPa after 5 freeze-thaw cycles respectively. [44] In conclusion, the robust performance of the core-shell structured cellulose-based hydrogels during consecutive freeze-thaw cycles emphasizes their reusability in coolant applications.

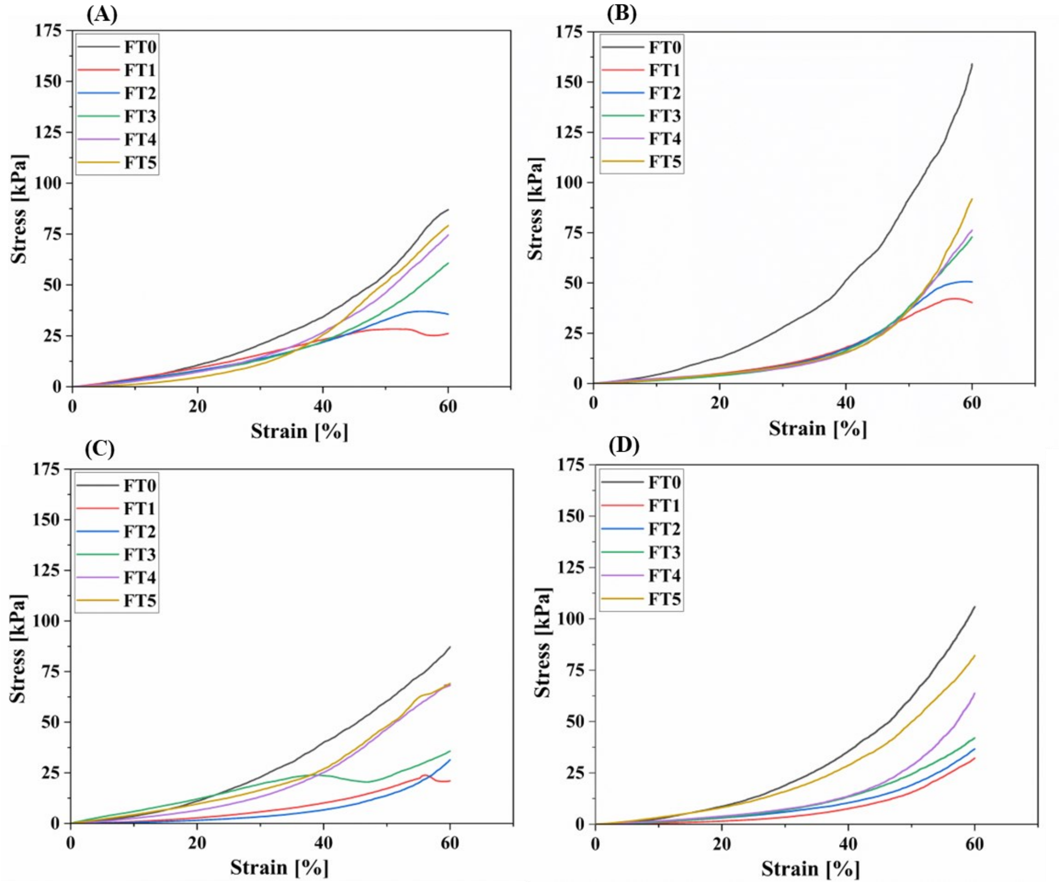

Figure 3.3 Compressive stress-strain curves of cellulose-based hydrogels before and after freeze-thaw cycles: (A) C2A5Cl, (B) C2A10Cl, (C) CA2A5Cl, and (D) CA2A10Cl.

3.3.2.1 Water retention capacity on rehydration

The water retention capacity of cellulose-based hydrogels after freeze-thaw cycles was analyzed. All the presented hydrogels were hydrophilic in nature and possessed the innate ability to rehydrate in water for reuse. As shown in **Figure 4**, with the increase in the number of freeze-thaw cycles, the water uptake in all the hydrogels gradually reduced, which might be attributed to the formation of denser matrices with more physical crosslinks. As expected, the addition of alginate in the hydrogel networks enhanced the water retention capacity. The CA2A10Cl hydrogel possessed the highest water-uptake of 97.4% after 1 freeze-thaw cycle and remained to be of 88.8% after 5 freeze-thaw cycles. Similarly, CA2A5Cl also had a higher water content of 80.1% compared to those of C2A5Cl (68.9%) and C2A10Cl (72.2%) hydrogels. This was due to the presence of the -COO^- groups of alginate that enhanced the ability of the hydrogels to absorb and retain more water. [45, 46] In comparison with other hydrogel coolants, the cellulose-based hydrogels demonstrated comparable water retention capacity. The previously reported gelatin-based hydrogel displayed a decrease in the average total water content from 89.38% to 84.46% after 5 freeze-thaw cycles. [27] In another study, the water contents of both gelatin and gelatin/menadione sodium bisulfite hydrogels ranged between 84.9-88.6% before freeze-thaw treatments and retained 82.3- 86.5% after 10 freeze-thaw cycles. [44]

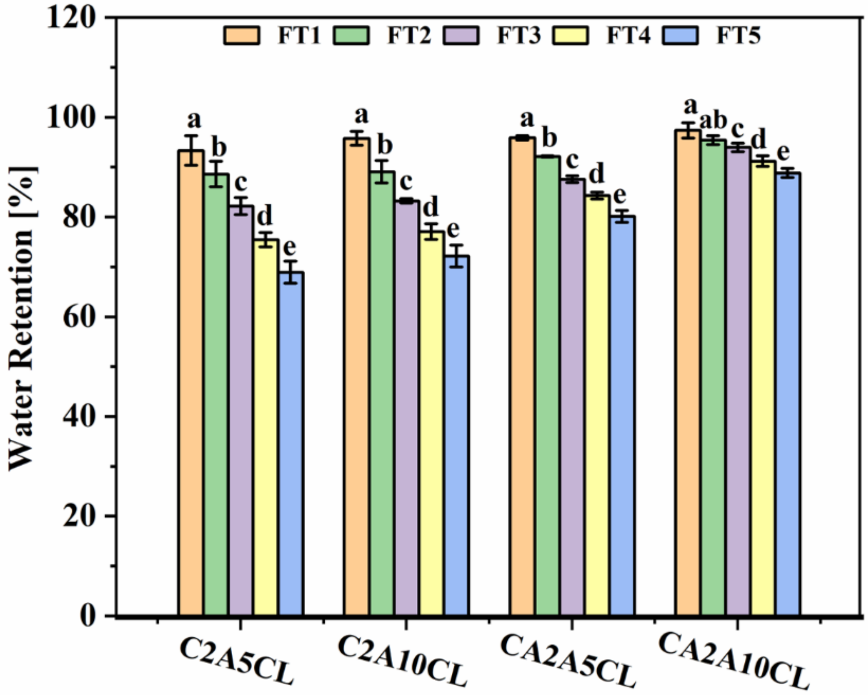

Figure 3.4 Water retention capacity on rehydration of cellulose-based hydrogels after freeze-thaw cycles. *Different letters on the top of columns represented the significant difference after freeze-thaw treatment ($p < 0.05$).

3.3.2.3. Latent heat of fusion

The heat-absorbing capacity of cellulose-based hydrogels before and after freeze-thaw treatment was studied. The characteristic peaks at about 0 °C mark the phase transition from ice to water, which is an important aspect for understanding the behavior of the hydrogels as a coolant in maintaining food at optimal temperature. The freezable water content is correlated with the endothermic region at around 0 °C, [47] and it has been reported that the conventional ice cubes had a latent heat of fusion of 334.5 J/g at 0 °C. [48] As shown in **Figure 5**, all the formulated hydrogels demonstrated the similar phase transition profiles. The C2A5Cl hydrogel, possessed the transition temperature of -0.47 °C and the latent heat of fusion of 305.9 J/g, while C2A10Cl, CA2A5Cl, and CA2A10Cl hydrogels had the lower transition temperatures and latent heat values. It might be due to the disrupted hydrogen bonding by the presence of polymer matrix, which could reduce the energy required for phase transition from solid to liquid state. [49, 50] In addition, higher crosslinking degree of hydrogels could contribute to the reduced latent heat of fusion, [51, 52] so the increase in Ca^{2+} ion concentration in the coating solution led to the reduced latent heat values. After 5 freeze-thaw cycles, the C2A5Cl, C2A10Cl, CA2A5Cl, and CA2A10Cl hydrogels showed a slight decrease in the latent heat of fusion by 10.7%, 12.3%, 7.0%, and 6.6%, respectively. This could be due to the loss of freezable water content within the hydrogels as it was revealed in the water retention test. The cellulose-based hydrogels demonstrated higher latent heat of fusion values than the other reported hydrogels. For example, the cornstarch hydrogels possessed a latent heat of fusion of 254.6 J/g before freeze-thaw treatments, [29] while the gelatin hydrogels experienced a substantial decrease in latent heat from 265.4 J/g to 171.9 J/g after five freeze-thaw cycles. [27]

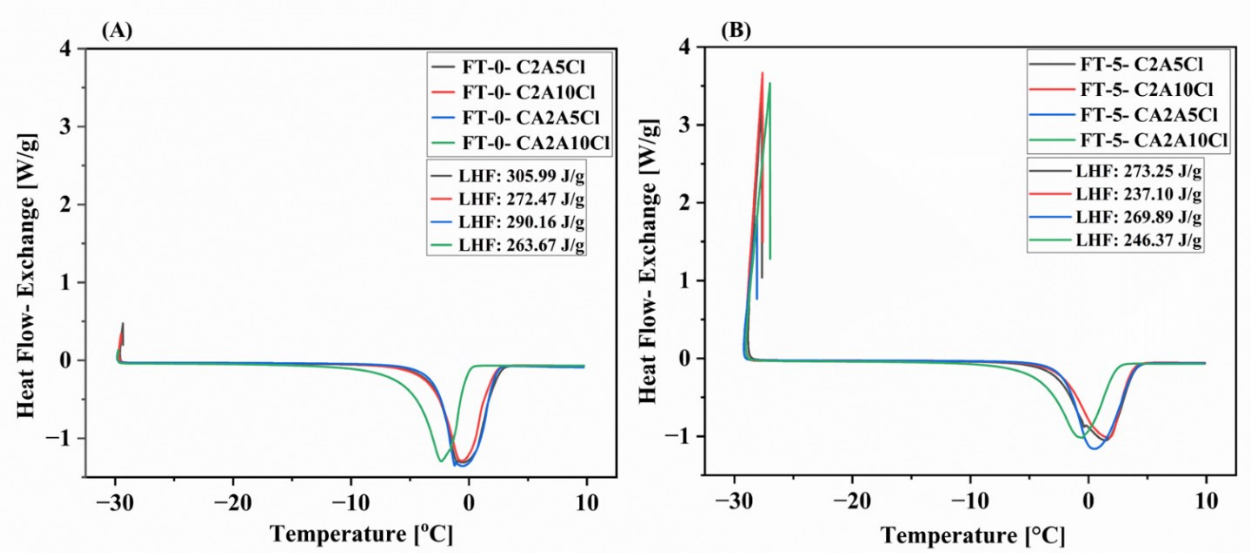

Figure 3.5 Latent heat of fusion (LHF) of cellulose-based hydrogels (A) before and (B) after 5 freeze-thaw cycles.

3.3.3 Comparison study of conventional ice cubes and C2A10Cl hydrogels

Understanding the thermal characteristics of hydrogel coolants is critical for optimizing their functionalities and their applicability in various fields. The thawing behavior of a coolant system plays a vital role in influencing the cold chain and food storage management. The C2A10Cl hydrogel had the best overall properties including mechanical strength, water retention, and latent heat value, so it was selected to compare with the conventional ice cubes. As shown in **Figure 6** (A), conventional ice cubes and C2A10Cl, both frozen at -20 °C and placed at room temperature, presented similar thawing patterns, reflecting the comparable capacity of C2A10Cl to retain and release thermal energy. Also, it is noteworthy that the C2A10Cl hydrogel did not generate any meltwater when thawed, in converse to the conventional ice cubes. Hence, this attractive feature could provide a safer environment that is crucial for limiting microbial cross-contamination.

The effectiveness of cooling perishable goods to below 4 °C (referred to the safe food handling temperature boundary), is a significant factor that influences the freshness and spoilage rate of food. [53] Both the conventional ice cubes and C2A10Cl displayed a similar cooling trend by gradually reducing the temperature of the blueberries. The conventional ice cubes could chill the blueberries to 4 °C within 26 minutes, whereas the same amount of C2A10Cl hydrogel achieved the threshold temperature of below 4 °C within 32 minutes.

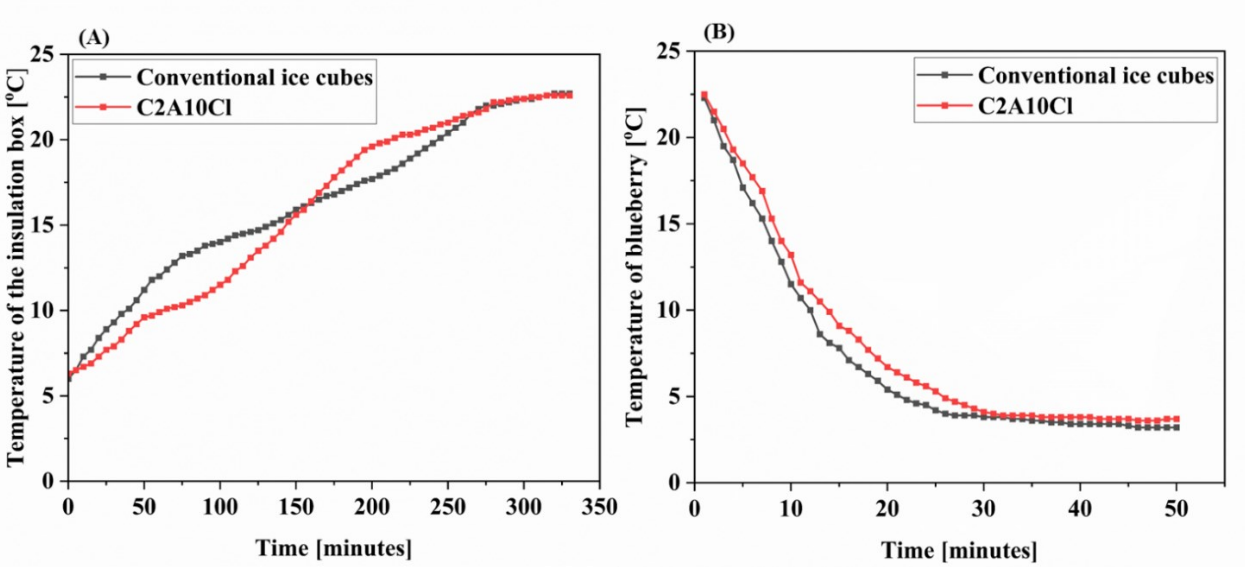

Figure 3.6 (A) Thawing curves and (B) cooling curves of conventional ice cubes and C2A10Cl hydrogels.

3.4 CONCLUSION

The waste cotton fabrics were successfully recycled into cellulose-based hydrogels with a special core-shell design to be used as a sustainable and effective food coolant. All resultant cellulose-based hydrogels displayed desirable characteristics such as good water retention property, high latent heat value, good reusability, and especially high compressive strength owing to their core-shell structures. Notably, the C2A10Cl hydrogel had mechanical strength of 144.7 kPa and efficient water retention that were better than the previously reported sustainable coolants, while their thawing and cooling performances were comparable to the conventional ice cubes without any meltwater generation. Therefore, this work reveals the potential to recycle cellulosic waste into sustainable products and suggests a feasible strategy to rationally design high-performance food coolants.

3.5 EXPERIMENTAL SECTION

3.5.1 Materials

Waste cotton clothes were kindly provided by Renaissance (Montreal, Canada). Sulfuric acid (95.0%−98.0%), epichlorohydrin (≥99.0%), and sodium alginate were purchased from Millipore-Sigma (Oakville, ON, Canada). Sodium hydroxide (≥97.0%), urea (≥99.6%) and calcium chloride anhydrous (93%) were purchased from Fisher Scientific (Ottawa, ON, Canada).

3.5.2 Preparation of cellulose-based hydrogels

A desired amount of cotton fibers from the collected waste cotton cloths was immersed in (30 wt%) H_2SO_4 solution and stirred at 200 rpm and 25°C for 48 h to decrease the molecular weight of cellulose. After that, the fibers were washed with deionized water and dried in the oven at 50 °C for 24 h. [54] Cellulose fibers and alginate were added to NaOH (7 wt%)/ urea (12 wt%) aqueous solutions precooled at -12 °C and stirred at 2,000 rpm for 8 minutes. [55] Subsequently, epichlorohydrin (10 wt%) was added dropwise into the solutions, stirred for 10 minutes, and heated at 60 °C until gelation. The hydrogels were washed in distilled water and then immersed in alginate (2 w/v%) solution for 12 hours, and then transferred into $CaCl_2$ (2 w/v%) solution for another 12 hours to form the core-shell structure. The compositions of cellulose-based hydrogels and coating solutions are listed in **Table 1**.

Table 3.1 Compositions of cellulose-based hydrogels.

Samples	**Core composition**		**Shell composition**	
	Cellulose content (wt %)	Alginate content (wt %)	Alginate content (wt %)	$CaCl_2$ content (wt %)
C2A5Cl	5	0	2	5
C2A10Cl	5	0	2	10
CA2A5Cl	4	1	2	5
CA2A10Cl	4	1	2	10

3.5.3 Characterization

3.5.3.1 Cellulose-based hydrogel morphology

Scanning electron microscopy (SEM) was employed to study the morphology of cellulose-based hydrogels. The samples were freeze-dried and subjected to 4 nm gold-platinum sputtering through the Leica EM ACE200 low vacuum coater (Vaughan, ON, Canada). The surface and cross-section of cellulose-based hydrogels were observed by a SEM Hitachi TM-1000, Japan.

3.5.3.2 Cellulose-based hydrogel properties

3.5.3.2.1 Mechanical strength

The compressive tests of cellulose-based hydrogels before (FT-0) and after each freeze-thaw cycle (FT-1 to FT-5) were carried out utilizing a compact tabletop universal tester (ADMET eXpert

7601, Norwood, MA, USA) equipped with a 250 lb load cell. Each cylindrical hydrogel sample (diameter of 1.3 cm and height of 5.0 mm) was compressed at a rate of 0.5 mm/min to 60% of sample height. The compressive strength was recorded, and each test was repeated three times.

3.5.3.2.2 Water retention capacity

The water retention test was carried out to study the stability of cellulose-based hydrogels after the freeze-thaw cycles. Before subjecting to freeze-thaw treatment, the initial weights (W_0) of hydrogels were measured. After each freeze-thaw cycle, the hydrogels were rehydrated in distilled water for 30 minutes and wiped gently to remove the surface water. Their weights (W_t) were measured, and the water retention capacity was calculated according to the following equation:

$$W_L\ \% = \frac{(W_0 - W_t)}{W_0} * 100 \tag{1}$$

$$W_R = 100 - W_L \tag{2}$$

where, W_L is defined as the water loss %, and W_R is the water retention % after rehydration.

3.5.3.2.3 Latent heat of fusion

The cellulose-based hydrogels before and after freeze-thaw treatment were sealed inside the Tzero-aluminum pans with hermetic lids and tested by DSC 2500 discovery (TA Instruments, New Castle, Delaware) from -30 °C to 10 °C with a 1 °C/min heating rate under a 50 mL/min protective nitrogen flow.

3.5.4 Comparison study of conventional ice cubes and cellulose-based hydrogels

3.5.4.1 Thawing behavior

The conventional ice cubes and C2A10Cl hydrogel, both with the same cylindrical measurements of 1 cm height and 1.3 cm diameter were frozen at -20 °C. Equal amounts (13 grams) of ice cubes and C2A10Cl hydrogel were placed at the bottom of two identical insulation boxes (4.5 cm × 5.8 cm × 3.8 cm). The temperature of the atmosphere inside the insulation boxes was monitored by thermometers and recorded.

3.5.4.2 Cooling effect on blueberries

The conventional ice cubes and C2A10Cl hydrogel, both with the dimensional measurements of 1 cm in height and 1.3 cm in diameter, were frozen at -20 °C. Equal amounts (13 grams) of ice cubes and C2A10Cl hydrogels were placed evenly to cover the entire bottom of two identical insulation boxes 4.5 cm × 5.8 cm × 3.8 cm. Blueberries (13 grams) were placed on the coolants, and the temperature of the blueberries was measured by positioning the thermometers at the top of the blueberries. The cooling curves of the blueberries were recorded.

3.5.5 Statistical Analysis

The statistical assessment was conducted by analysis of variance (ANOVA), along with multiple-comparison tests using Duncan's multiple-range test at the 95% confidence level. All the analyses were performed by using SPSS statistical software (version 22.0, IBM, New York, USA) with a probability of $p < 0.05$ considered to be significant.

Author Contributions

S. P. performed methodology, investigation, formal analysis, data curation, validation and wrote the original draft. Y. Z. performed validation, review of the project and draft. Y. W. performed conceptualization, review and edit of the draft and supervision.

Acknowledgements

The work was supported by the Natural Sciences and Engineering Research Council of Canada (NSERC RGPIN-2019-04498, NSERC DGECR-2019-00472). S. P. would like to thank the support of Institut sur la nutrition et les aliments fonctionnels (INAF). Y. Z. would like to thank the support of China Scholarship Council (CSC NO. 202107970010).

Conflict of Interest

The authors declare no conflict of interest.

Data Availability Statement

The data that support the findings of this study are available on request from the corresponding author.

Ethical Statement

The research described in this manuscript does not include animal experiments or human subjects or tissue samples from human subjects.

3.6 REFERENCES

[1] N. Nodali, H.-I. Hsiao, J. Vlajic, M.-F. Yang, H.-T. V. Lin, *Food Control* **2018**, *89*, 12-21.

[2] A. Thakali, J. D. MacRae, *Environ. Res.* **2021**, *194*, 110635.

[3] C. Rajeh, I. P. Saoud, S. Kharroubi, S. Naalbandian, M. G. Abiad, *J. Mater. Cycles Waste Manage* **2021**, *23*, 1-17.

[4] W. DeFlorio, S. Liu, A. R. White, T. M. Taylor, L. Cisneros-Zevallos, Y. Min, E. M. A. Scholar, *Compr. Rev. Food Sci. Food Saf.* **2021**, *20*, 3093-3134.

[5] M. Calati, K. Hooman, S. Mancin, *Int. J. Thermofluids* **2022**, *16*, 100224.

[6] L. Filina-Dawidowicz, S. Filin, *Energy Efficiency* **2019**, *12*, 1151-1165.

[7] U. S. K. Madduma-Bandarage, S. V. Madihally, *J. Appl. Polym. Sci.* **2021**, *138*, 50376.

[8] J. Yang, Y. Chen, L. Zhao, J. Zhang, H. Luo, *Polym. Rev.* **2023**, *63*, 574-612.

[9] D. Hu, M. Zeng, Y. Sun, J. Yuan, Y. Wei, *SusMat* **2021**, *1*, 266-284.

[10] Y. Cong, J. Fu, *Langmuir* **2022**, *38*, 11503-11513.

[11] G. Bovone, O. Y. Dudaryeva, B. Marco-Dufort, M. W. Tibbitt, *ACS Biomater. Sci. Eng.* **2021**, *7*(9), 4048-4076.

[12] G. Janarthanan, I. Noh, *J. Mater. Sci. Technol.* **2021**, *63*, 35-53.

[13] J. Leppiniemi, P. Lahtinen, A. Paajanen, R. Mahlberg, S. Metsa-Kortelainen, T. Pinomaa, H. Pajari, I. Vikholm-Lundin, P. Pursula, V. P. Hytonen, *ACS Appl. Mater. Interfaces* **2017**, *9*(26), 21959-21970.

[14] N. A. Peppas, A. G. Mikos, *Hydrogels Med Pharm*, CRC press, 2019.

[15] P. Mehta, M. Sharma, M. Devi, *J. Mech. Behav. Biomed. Mater.* **2023**, 106145.

[16] W. Wang, R. Narain, H. Zeng, *Polym Sci Nanotechnol*, Elsevier, 2024, Ch. 10.

[17] P. Lu, Y. Yang, R. Liu, X. Liu, J. Ma, M. Wu, S. Wang, *Carbohydr. Polym.* **2020**, *249*, 116831.

[18] F. Ávila-Salas, A. Marican, S. Pinochet, G. Carreño, O. Valdés, B. Venegas, W. Donoso, G. Cabrera-Barjas, S. Vijayakumar, E. F. Durán-Lara, *Pharmaceutics* **2019**, *11*(9), 447.

[19] R. S. Dassanayake, S. Acharya, N. Abidi, *Adv. Sorption Process Appl.*, 2018, Ch. 1.

[20] SM F. Kabir, P. P. Sikdar, B. Haque, MA R. Bhuiyan, A. Ali, M. N. Islam, *Prog. Biomater.* **2018**, *7*, 153-174.

[21] B. Baghaei, M. Skrifvars, *Molecules* **2020**, *25*(12), 2836.

[22] N. Abidi, M. Manike, *Textile Res. J.* **2018**, *88*(7), 719-730.

[23] M. A. Khan, A. Wahid, M. Ahmad, M. T. Tahir, M. Ahmed, S. Ahmad, M. Hasanuzzaman, *Cotton production and uses: Agronomy, crop protection, and postharvest technologies*, 2020, Ch. 1.

[24] L. Lu, W. Fan, X. Meng, L. Xue, S. Ge, C. Wang, S. Y. Foong, et al., *Sci. Total Environ.* **2023**, *856*, 158798.

[25] C. Zhou, Y. Wang, *J. Appl. Polym. Sci.* **2021**, *138*(48), 51255.

[26] F. Wang, Y. Zhang, Y. Wang, *ACS Omega* **2021**, *6*(50), 34314-34326.

[27] J. Zou, L. Wang, G. Sun, *ACS Sustainable Chem. Eng.* **2021**, *9*(46), 15357-15364.

[28] J. Zou, L. Wang, G. Sun, *ACS Sustainable Chem. Eng.* **2021**, *9*(46), 15365-15374.

[29] Y. Zheng, Y. Ma, R. H. Ukwatta, F. Xue, C. Li, *Polymers* **2024**, *16*(5), 569.

[30] S. Radoor, J. Karayil, A. Jayakumar, D. R. Kandel, J. T. Kim, S. Siengchin, J. Lee, *Carbohydr. Polym.* **2023**, 121339.

[31] S. Zhang, Y. Wan, W. Yuan, Y. Zhang, Z. Zhou, M. Zhang, L. Wang, R. Wang, *Polymers* **2022**, *14*(1), 212.

[32] J. Zou, L. Wang, G. Sun, *ACS Appl. Mater. Interfaces* **2023**, *15*(28), 34087-34096.

[33] C. Chang, B. Duan, L. Zhang, *Polymer* **2009**, *50*(23), 5467-5473.

[34] H. Lu, J. A. Butler, N. S. Britten, P. D. Venkatraman, S. S. Rahatekar, *Nanomaterials* **2021**, *11*(8), 2062.

[35] N. Che, N. Fitrah, N. Zainuddin, M. Ahmad, *Pertanika J. Sci. Technol.* **2019**, *27*(1), 489 - 498.

[36] C. M. Hassan, N. A. Peppas, *Macromolecules* **2000**, *33*(7), 2472-2479.

[37] H. Qin, Y. Zhang, J. Jiang, L. Wang, M. Song, R. Bi, P. Zhu, F. Jiang, *Adv. Funct. Mater.* **2021**, *31*(46), 2106269.

[38] P. Kaur, H. B. Bohidar, D. R. Nisbet, F. M. Pfeffer, A. Rifai, R. Williams, R. Agrawal, *Cellulose* **2023**, *30*(5), 2713-2730.

[39] S. Feng, J. Yi, Y. Ma, J. Bi, *Food Chem.* **2023**, *428*, 136758.

[40] Y. Wang, Y. Xue, J. Wang, Y. Zhu, Y. Zhu, X. Zhang, J. Liao, et al., *Polymers* **2019**, *11*(7), 1112.

[41] H. Xu, F.-K. Shi, X.-Y. Liu, M. Zhong, X.-M. Xie, *Soft Matter* **2020**, *16*(18), 4407-4413.

[42] K. Wu, H. Han, L. Xu, Y. Gao, Z. Yang, Z. Jiang, G. D. Schutter, *Constr. Build. Mater.* **2021**, *291*, 123274.

[43] S. Feng, J. Bi, J. Yi, X. Li, J. Lyu, Y. Guo, Y. Ma, *Food Res. Int.* **2022**, *159*, 111555.

[44] J. Zou, A. O. Sbodio, B. Blanco-Ulate, L. Wang, G. Sun, *Adv. Funct. Mater.* **2022**, *32*(26), 2201347.

[45] Z. Yu, J. Liu, H. He, S. Ma, J. Yao, *Carbohydr. Polym.* **2021**, *255*, 117485.

[46] Y. Wang, A. Jiao, C. Qiu, Q. Liu, Y. Yang, S. Bian, F. Zeng, Z. Jin, *Food Hydrocolloids* **2022**, *131*, 107737.

[47] S. Abasi, R. Davis Jr, D. A. Podstawczyk, A. Guiseppi-Elie, *Polymer* **2019**, *185*, 121978.

[48] Y. Liu, B. Xu, Y. Li, S.-Y. Quek, K. Huang, *Adv. Sci.* **2024**, *2309753*.

[49] X. Huang, L. Wang, K. Liu, L. Liao, H. Sun, J. Wang, X. Tian, et al., *Nature* **2023**, *617*(7959), 86-91.

[50] S. Snigdha, N. Kalarikkal, S. Thomas, E. K. Radhakrishnan, in *Nano Hydrogels: Physico-Chemical Properties and Recent Advances in Structural Designing* **2021**, 127-133.

[51] W.-C. Jao, H.-C. Chen, C.-H. Lin, M.-C. Yang, *Polym. Adv. Technol.* **2009**, *20*(8), 680-688.

[52] L. Liu, X. Zou, Y. Wang, W. Zhou, J. Shi, Y. Ye, Y. Zhao, et al., *Polymer* **2021**, *223*, 123710.

[53] R. Owusu-Apenten, E. Vieira, *Elementary Food Science* **2023**, 197-215.

[54] Y. Chu, C. Popovich, Y. Wang, *Compos. Part C: Open Access* **2023**, *12*, 100390.

[55] O. Aarstad, E. B. Heggset, I. S. Pedersen, S. H. Bjørnøy, K. Syverud, B. L. Strand, *Polymers* **2017**, *9*(8), 378.

CONNECTING STATEMENT II

In **Chapter 3**, the dip-coated cellulose-based hydrogels displayed notable mechanical strength, good water retention, and remarkable latent heat of fusion characteristics. It was significant to note that the cooling and thawing behaviors of the C2A10Cl hydrogel resembled the conventional ice cubes, suggesting similarity in their performance as a coolant. In **Chapter 4**, the cellulose-based hydrogels were further modified by the incorporation of antibacterial agents such as nisin and lysozyme. The effects of nisin and lysozyme on cellulose-based hydrogel properties were investigated to evaluate the potential as antibacterial coolants.

CHAPTER 4. DEVELOPMENT OF NOVEL ANTIBACTERIAL-INFUSED CELLULOSE HYDROGELS AS SUSTAINABLE FOOD COOLANTS FOR MICROBIAL CONTAMINATION REDUCTION

4.1 ABSTRACT

Microbial contamination of food products is a major challenge to food industry, leading to food spoilage and wastage, thus, there is a demand for the development of an ideal coolant. While the previously fabricated cellulose-based hydrogels reduced the generation of meltwater, they still could pose risks of microbial contamination. In this study, novel antibacterial cellulose-based hydrogels with a special core-shell configuration were synthesized as potential food coolants with high water retention and antibacterial properties. Sufficient mechanical and high-water retention properties of the unique core-shell designed-hydrogels were achieved by using cellulose hydrogel crosslinked with epichlorohydrin as the core and alginate/calcium chloride (ALG/$CaCl_2$) as the shell. The structure and properties of the synthesized hydrogels were characterized by Fourier transform infrared spectroscopy (FTIR), scanning electron microscopy (SEM), and compressive test. The antibacterial compounds, nisin (N) and lysozyme (L), were embedded in the oxidized cellulose (OXCL) hydrogels to eliminate the bacterial proliferation and potentially reduce cross-contamination issues of food products. The antibacterial activities were tested through the disc diffusion method against *Escherichia coli* and *Staphylococcus aureus*. Therefore, this newly developed antibacterial cellulose-based hydrogel derived from biomass waste offers a sustainable solution to food spoilage, having the potential to act as an efficient food coolant.

Keywords: Cellulose hydrogels, nisin, lysozyme, antibacterial property, meltwater.

4.2 INTRODUCTION

Food insecurity remains a major global challenge, with nearly $1/9^{th}$ of the population being food insecure, despite the exponential growth in food production. [1] One of the important factors influencing food wastage is the temperature at which the food products are maintained. Due to the lack of proper storage conditions, approximately 12% of food wastage occurs in the USA. [2] With the rapid increase in food production, there is a parallel amplification in the magnitude of food safety concerns. Inefficient temperature management, poor cold storage, and microbial contamination are some of the pivotal factors contributing to the loss of fresh produce [3]. As mentioned in the previous chapter, the main issue with the usage of conventional ice cubes is the cross-contamination and spread of harmful microbes to the fresh foods occurring through the meltwater transfer. Other drawbacks include the inability of the ice cubes to support optimal temperature to the food products after they melt, rendering them non-reusable, as well as increasing the wastage of water resources.

Hydrogels are intricate three-dimensional polymeric frameworks, known for their exceptional hydrophilicity, which can be constructed by both physical and chemical crosslinking techniques [4]. Hydrogels have gained significant interest among researchers and have been extensively investigated in the applications of functional food, food packaging, drug delivery, food safety, and other industrial applications [5-7]. Currently, there is a rising awareness regarding the importance and mounting demand for using biodegradable materials procured from renewable sources [8]. Cellulose is a predominant natural polymer with abundant hydroxyl groups and remarkable features such as affordability, renewability, sustainability, and non-toxicity [9]. The escalating consumption of cotton textiles has led to the simultaneous accumulation of waste cotton fabrics, and most of them are disposed into landfills or incinerated, which not only generates environmental pollution but also results in significant resource wastage [10,11].

In our previous work, cellulose-based hydrogels with robust compressive strength, good water retention ability, rehydration capacity, and efficient latent heat property have been developed, which demonstrated good physical resilience to freeze-thaw treatments. It will be more useful if the hydrogels can be endowed with antibacterial attributes for protecting both the hydrogel and its surrounding environment from microbial contamination. Nisin is a natural peptide produced by *Lactococcus lactis subsp.* with high antibacterial activity against Gram-positive bacteria and is widely used in food industry as a preservative, approved by the European Food Safety Authority and accepted as a food additive by both the US Food and Drug Administration and the World Health Organization [12]. Additionally, lysozyme, a monomeric protein, used in pharmacology and food industry, has relatively narrow antibacterial spectrum with instability and easy inactivation, making the practical application of free lysozyme quite limited [13]. Thus, chemical crosslinking of the antibacterial compounds such as nisin and lysozyme to the cellulose-based hydrogels through the Schiff base reaction could result in sustained release of the antibacterial agents, reducing their desorption and providing a long-term antibacterial activity [14]. In this study, a facile method to develop nisin and lysozyme anchored cellulose-based hydrogels, sourced from the post-consumer cotton textile, with a potential application as food coolants with reduced meltwater occurrence is presented. The properties of the antibacterial coolants were investigated by Fourier transform infrared spectroscopy (FTIR), scanning electron microscopy (SEM), compressive test and water retention test. Further, the antibacterial activity of the modified cellulose-based hydrogels were tested against both the Gram-positive bacteria, *Staphylococcus aureus* and the Gram-negative bacteria, *Escherichia coli*.

4.3. MATERIALS AND METHODS

4.3.1 Reagents and Materials

Waste cotton clothes were kindly provided by Renaissance (Montreal, Canada). Sulfuric acid (95.0%−98.0%), epichlorohydrin (≥99.0%), and sodium alginate was purchased from Millipore-Sigma (Oakville, ON, Canada). Sodium hydroxide (≥97.0%), sodium periodate (≥ 99.0%), urea (≥99.6%), anhydrous calcium chloride (93%), nisin, and lysozyme were purchased from Fisher Scientific (Ottawa, ON, Canada). Phosphate-buffered saline (10× PBS) was obtained from VWR International (Mississauga, ON, Canada).

4.3.2 Preparation of Antibacterial Hydrogels

The pretreatment of the waste cotton fabrics was performed by using 30 wt% sulfuric acid aqueous solution for 48 hours and stirred at 2000 rpm [15]. The cellulose fibers were then washed with distilled water until neutral pH was attained and oven-dried at 50 °C for 24 hours [16]. Cellulose fibers were dissolved in precooled NaOH (7 wt%)/ urea (12 wt%)/ distilled water (81 wt%) and stirred at 2,000 rpm for 8 mins. Epichlorohydrin was added and heated at 60 °C until cellulose hydrogels were formed [17]. The formed hydrogels were washed using distilled water and immersed in alginate (2 w/v%) solution for 12 hours, and then transferred into $CaCl_2$ (2 w/v%) solution for another 12 hours to form the core-shell structure. Further, the core-shell cellulose hydrogels were immersed in 5% (w/v) sodium periodate for 30 minutes to form oxidized hydrogels [18]. Finally, these hydrogels were immersed in either 2.5 mg/ml nisin PBS solution (pH 7.4) or 2.5 mg/ml lysozyme PBS solution (pH 7.4) [19,20]. The compositions of antibacterial cellulose-based hydrogels are listed in **Table 4.1**.

Table 4.1 Compositions of antibacterial cellulose-based hydrogels.

Samples	**Core composition**	**Shell composition**		**Sodium periodate** (w/v%)	**Antibacterial compound** (mg/ml)
	Cellulose content (wt %)	Alginate content (wt %)	$CaCl_2$ content (wt %)		
OXCL	5	2	10	5	0
OXCL-N	5	2	10	5	2.5
OXCL-L	5	2	10	5	2.5

4.3.3 Characterization

4.3.3.1 Cellulose Hydrogel Structure

4.3.3.1.1 Fourier transform infrared spectroscopy

FTIR analysis is used to determine the functional groups present in the hydrogels. The structure of the OXCL, OXCL-L, and OXCL-N hydrogels were characterized by FT-IR spectrometer (Cary 630, Agilent Technology, Santa Clara, CA, USA). The wavenumber range was 800-4000 cm^{-1} with a resolution of 2 cm^{-1}. To quantitatively analyze the data, the software Origin 2024 was used to normalize the spectra obtained and graphically represent them.

4.3.3.1.2 Scanning electron microscope

The morphology and structure of hydrogels were investigated by using scanning electron microscopy (SEM). Initial preparation involved cutting the samples into small parts and then freeze-drying them via lyophilization. Prior to observation, the samples were coated with a 4 nm gold-platinum sputtering process using the Leica EM ACE200 low vacuum coater (Vaughan, ON, Canada). Finally, the morphology of the shell and the cross-section were observed using SEM (Hitachi TM-1000, Japan).

4.3.3.2 Cellulose Hydrogel Properties

4.3.3.2.1 Mechanical strength

The compressive tests of hydrogels were performed by the texture analyzer (ADMET eXpert 7601, Norwood, MA, USA) equipped with a 250 lb load cell at a rate of 0.5 mm/min. The hydrogels with a radius of 6.5 mm and a height of 5.0 mm were compressed until 60% of the original height, and each sample was characterized using triplicates.

4.3.3.2.2 Water-retention capacity

The water retention of hydrogels during the freeze-thaw treatment was investigated. The original weight of the hydrogels (W_0) was measured before freeze-thaw treatment. After each freeze-thaw cycle, the hydrogels were rehydrated in distilled water for 30 minutes. The excess water on the surface was gently removed, and the weight (W_t) was measured. The water retention capacity after each cycle was calculated based on the following formula:

$$W_L \,\% = \frac{(W_0 - W_t)}{W_0} * 100 \tag{1}$$

$$W_R = 100 - W_L \tag{2}$$

where W_L is the water loss %, and W_R denotes water retention % after rehydration.

4.3.4 Antibacterial assay

The antibacterial assay was performed according to previous studies with some modifications [21-25]. The antibacterial activity of the hydrogels was evaluated against the Gram-positive bacteria *Staphylococcus aureus* ATCC 25923 and the Gram-negative bacteria *Escherichia coli* ATCC 25922. Each bacterial strain was revived using the Tryptic Soy Broth (TSB) at 37 °C for 24 hours. Then, the activated bacterial strains were cultured in TSB for 24 hours and diluted to 10^8 CFU/mL. Further, a disc diffusion assay was performed by spreading 100 uL of bacterial suspension on the petri plates containing the Tryptic Soy Agar (TSA) and incubating at 37 °C for 10 mins. The wells (diameter of 1.3 cm- size of the hydrogels) were carved using a sterile borer and hydrogels were placed in the wells. The OXCL hydrogel without any antibacterial compound was employed as the control. The diameter of the bacterial inhibition zone was measured after 24 hours of incubation at 37 °C.

4.3.5 Statistical Analysis

The statistical analysis was carried out by employing analysis of variance (ANOVA) alongside Duncan's multiple-range test at a 95% confidence level to ascertain significance. SPSS statistical software (version 22.0, IBM, New York, USA) was employed for all analyses with statistical significance defined as $p < 0.05$.

4.4 RESULTS AND DISCUSSION

4.4.1 Cellulose Hydrogel Structure

4.4.1.1 Fourier transform infrared spectroscopy

As depicted in Figure 4.1, the FTIR spectra showed the characteristic infrared peaks of the shell layer - ALG/$CaCl_2$ coating, and the core structures of cellulose, OXCL, OXCL-N, and OXCL-L hydrogels, identified based on their specific functional groups. Firstly, in the shell layer, the main peak observed at around 3300 cm^{-1} was due to the O─H stretching of alginate [26]. The peaks related to asymmetric and symmetric stretching vibrations of free carboxyl (COO^{-}) groups occurred at 1595 cm^{-1} and 1420 cm^{-1}, respectively [27]. The peak vibration observed at 1020 cm^{-1} was due to the carboxylate (C−O−C) group stretching [28]. In the core structure of CL hydrogels, a broad spectrum at 3338 cm^{-1} was observed that corresponds to stretching vibration of a large number of hydroxyl groups, while peaks at 2874 cm^{-1} were attributed to C─H stretching [29]. A strong and sharp peak characterized as C=O appeared at 1594 cm^{-1} and the small peak of C−OH occurred at 1411 cm^{-1} [30]. The C−O−C pyranose ring skeletal vibration was characterized at 1018 cm^{-1} [31]. In OXCL hydrogel, the peak at 3350 cm^{-1} was attributed to stretching vibrations of the hydroxyl groups, [32] which was weaker than that in cellulose hydrogels due to the replacement of OH groups by the aldehyde groups, confirming the cellulose oxidation. The characteristic peak of C=O stretching vibration occurred at 1725 cm^{-1} [33]. The strong absorption peak at 1032 cm^{-1} might be due to the C–O stretching vibration in secondary alcohol, and the peak at 843 cm^{-1} was observed due to the presence of hemiacetal band [34]. The occurrence of the hemiacetal band was due to the interaction between aldehyde and hydroxyl groups [35]. Further, after oxidation, the aldehyde groups of OXCL could anchor with the amino groups of antibacterial compounds through the Schiff base reaction [36,37]. The confirmatory spectral region for the incorporated antibacterial compounds, nisin and lysozyme, was in the range of 1580-1720 cm^{-1} [38]. Compared to OXCL, two peaks with increased intensities were observed at 1614 cm^{-1} and 1644 cm^{-1} in OXCL-N and OXCL-L hydrogels, which were assigned to the C=N bands combined with N–H deformation, confirming the adherence of nisin and lysozyme [39-42]. The slight increase in the peak intensity at around 3000-3500 cm^{-1} could be due to stretching vibrations of N–H and O–H, attributed to the binding of nisin and lysozyme to OXCL [43], and the absorption peaks at 1732 cm^{-1} and 1736 cm^{-1} could be due to the reduced aldehyde groups [44]. Finally, the slight variation in the absorption peaks at around 1100 cm^{-1} could be ascribed to the C–N band of OXCL-N and OXCL-L hydrogels [45].

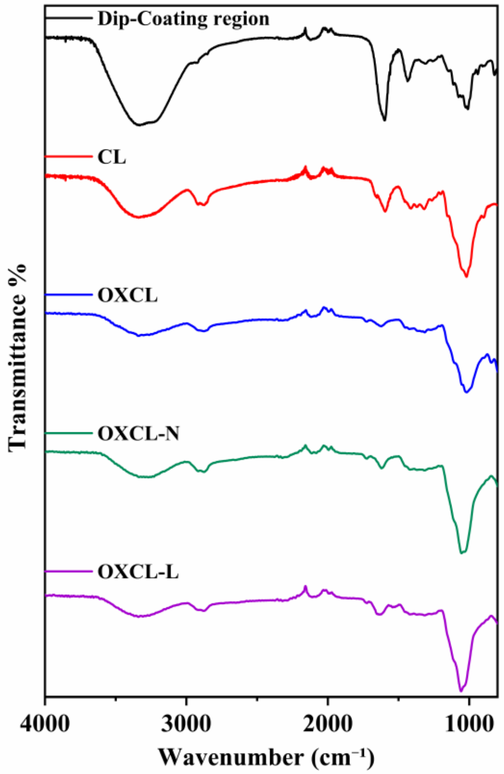

Figure 4.1 FTIR spectra of the dip-coated shell layer and core structures of CL, OXCL, OXCL-N, and OXCL-L hydrogels.

4.4.1.2 Morphology

Scanning electron microscopy (SEM) was employed to investigate the morphology of OXCL, OXCL-N, and OXCL-L hydrogels. A clear core-sheath morphology of the hydrogels was observed. Before freeze-thaw treatment, the OXCL hydrogels had a compact structure with very few large pores. The less pores in OXCL hydrogels could be attributed to the oxidation of cellulose with sodium periodate and the subsequent replacement of hydroxyl groups in the original cellulose structure by the aldehyde groups [46]. However, the morphology of OXCL-N and OXCL-L hydrogels appeared quite different with more pores due to the cross-linking of nisin and lysozyme with OXCL hydrogel via the Schiff base reaction. In OXCL-N hydrogels, the addition of nisin appeared as filament/small porous structures as indicated by the yellow marks which was also reported in the previous literature [47,48]. These additional filament/small pores in OXCL-N hydrogels could be due to the configuration of the OXCL hydrogels and the nisin molecules, causing less shrinkage of the network structure [49]. Similarly, the porous structure of OXCL-L hydrogels with lysozyme deposition indicated by the yellow marks was also due to the immobilization of lysozyme onto the OXCL hydrogel through the Schiff base reaction [50].

The shell layer appeared to be uniform with even morphology before and after the freeze-thaw cycles. The freeze-thaw treatments and the number of cycles had some influence on the core-shell structure of the hydrogels due to the syneresis phenomenon [51-53]. After the freeze-thaw treatment, the core structure of the hydrogels appeared to be considerably changed based on the composition of the hydrogels. Due to the growth of ice grains during freezing, OXCL hydrogels possessed more large pores, whereas the OXCL-N and OXCL-L hydrogels still retained the filamentous structure and small pores without much damage, which could be due to the additional Schiff-base interaction between nisin, lysozyme, and the OXCL hydrogels.

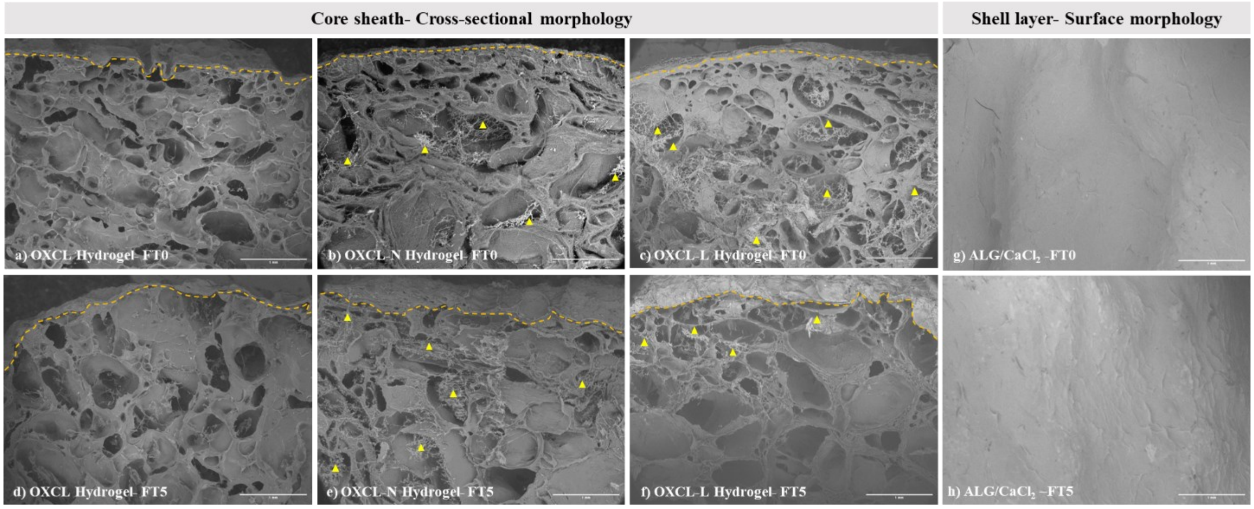

Figure 4.2 SEM images of cross-sections and surface morphology of OXCL, OXCL-N, and OXCL-L hydrogels before (upper) and after (below) five cycles of freeze-thaw treatment. *The doted lines indicate the shell layers, and the yellow marks represent deposition of nisin and lysozyme on their respective hydrogels. Scale bar: 1 mm.

4.4.2 Cellulose Hydrogel Properties

4.4.2.1 Mechanical strength

The effects of the incorporation of nisin and lysozyme, Ca^{2+} ion concentration and freeze-thaw treatment on the compressive strength of cellulose-based hydrogels were investigated. As observed in Figure 4.3 and Figure 4.4, the compressive strengths of OXCL, OXCL-L, and OXCL-N hydrogels before freeze-thaw treatment were 116.6 kPa, 127.1 kPa, and 142.8 kPa, and their compressive strains were around 52%, 45%, and 52%, respectively.

The freeze-thaw treatment exhibited a considerable effect on the mechanical properties of OXCL, OXCL-L and OXCL-N hydrogels. The compressive strengths of OXCL, OXCL-L, and OXCL-N hydrogels were 28.9 kPa, 32.7 kPa and 48.3 kPa respectively after a single freeze-thaw cycle. This might be due to the ice grain development and low physical crosslinking after the first cycle [42]. After 5 freeze-thaw cycles, the stability of the hydrogels improved with no breakage until 60% strain limit, and the compressive strengths of OXCL, OXCL-L, and OXCL-N hydrogels were 52.5 kPa, 79.1 kPa and 92.6 kPa respectively. This improvement could be ascribed to the Schiff base reaction, where the amine groups of nisin and lysozyme attached to the aldehyde groups presented in OXCL hydrogel network [39]. Also, the addition of nisin and lysozyme provided additional cohesion to the hydrogels and contributed to their improved strengths [49]. These results indicated that the increase in the number of freeze-thaw cycles provided a better stability to the network structure of hydrogels due to the generation of more physical crosslinking [49,52,53].

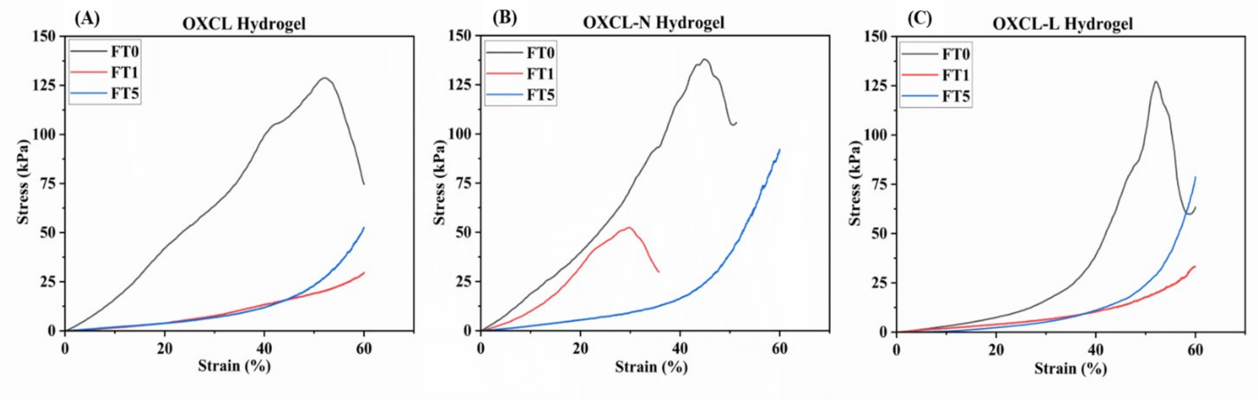

Figure 4.3 Compressive stress-strain curves of antibacterial cellulose-based hydrogels before and after freeze-thaw cycles: (A) OXCL, (B) OXCL-N, and (C) OXCL-L hydrogels.

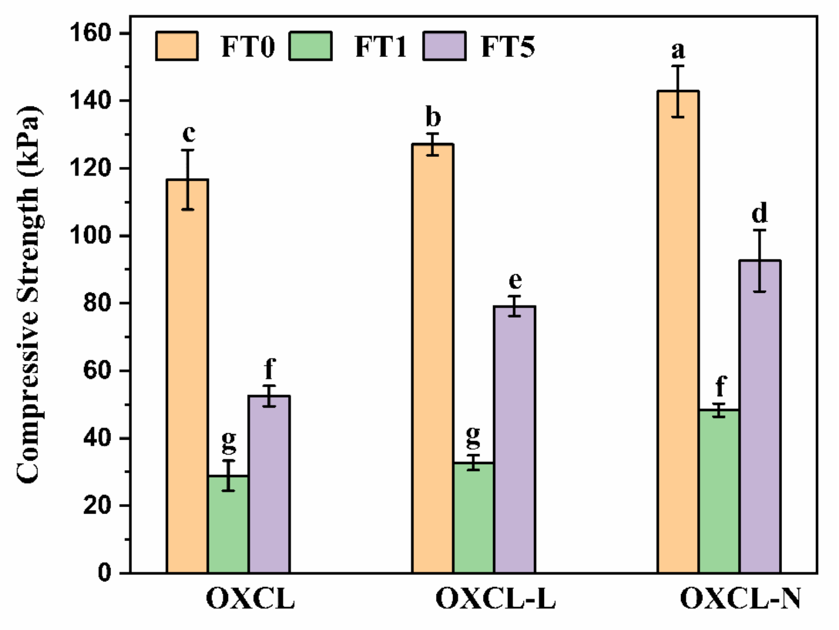

Figure 4.4 Compressive strength of antibacterial cellulose-based hydrogels before and after freeze-thaw cycles. *Different letters on the top of columns represents the significant difference between different samples for freeze-thaw treatments ($p < 0.05$).

4.4.2.2 Water retention capacity

One of the main prerequisites for hydrogels to function efficiently as a food coolant is their ability to retain a significant volume of water within their network and possess rehydration capacity over successive freeze-thaw cycles. Figure 4.5 demonstrates the water retention capacity of the OXCL, OXCL-N, and OXCL-L hydrogels. The OXCL hydrogel displayed the least water retention capacity of about 87.9% after 1 cycle, which could be due to the small pores and dense network [54]. The water retention of the OXCL was significantly reduced to 66.7% after 5 cycles. It could be explained that, with successive freeze-thaw cycles, syneresis occurred and altered the hydrogel's structure, resulting in compromised structural integrity and diminished water retention capacity [55]. The OXCL-N hydrogel possessed the highest water retention of about 81.1% after

5 cycles, which might be due to the incorporation of nisin [56,57]. During the rehydration process, the hydrophilic segments of nisin could interact with the water molecules and bind them [58]. Similarly, the water retention capacity of the OXCL-L hydrogels was 97.0% after freeze-thaw cycle 1, and was largely retained to 80.2% after 5 cycles, probably due to the hydrophilicity of lysozyme, that better trap the water molecules in the hydrogels [59,60].

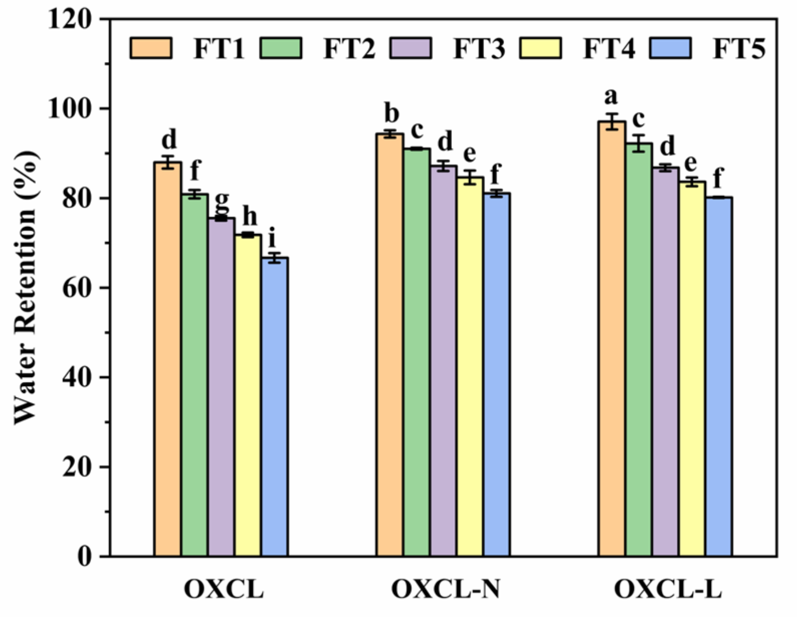

Figure 4.5 Water retention capacity on rehydration of antibacterial cellulose-based hydrogels after freeze-thaw cycles. *Different letters on the top of columns represented the significant difference between different samples after freeze-thaw treatment ($p < 0.05$).

4.4.3 Antibacterial Properties

The disc diffusion method was used to evaluate the antibacterial properties of OXCL, OXCL-N, and OXCL-L hydrogels. It was clearly observed that the OXCL-N and OXCL-L hydrogels exhibited high antibacterial activity against *S. aureus*. The mechanism involves the binding of nisin to lipid II of the Gram-positive bacteria, which results in pore formation and the outflow of the cell constituents [29]. Similarly, lysozyme is more active against Gram-positive bacteria, as it is capable of breaking down the β-1,4-glycosidic bond which acts as a linkage between N-acetylmuramic acid and N-acetylglucosamide in the polysaccharide backbone of the peptidoglycans of the cell walls [30]. As shown in Figure 4.6, the zone of inhibition of OXCL-N and OXCL-L hydrogels against *S. aureus* were 3.66 mm and 4.06 mm, respectively. Whereas only a small inhibition zone was observed for OXCL-N and OXCL-L hydrogels against *E. coli* (1.1 mm and 1.2 mm, respectively). This might be due to the presence of a protective lipopolysaccharides layer in the gram-negative bacteria, which prevents nisin from reaching the lipid layer [61]. Similarly, the lysozyme was blocked from the entry into the outer polysaccharide frameworks of the gram-negative bacteria [62]. The OXCL hydrogels showed no inhibitory zone against *E. coli* or *S. aureus*. This indicated that the antibacterial effects were caused by nisin and lysozyme only [48].

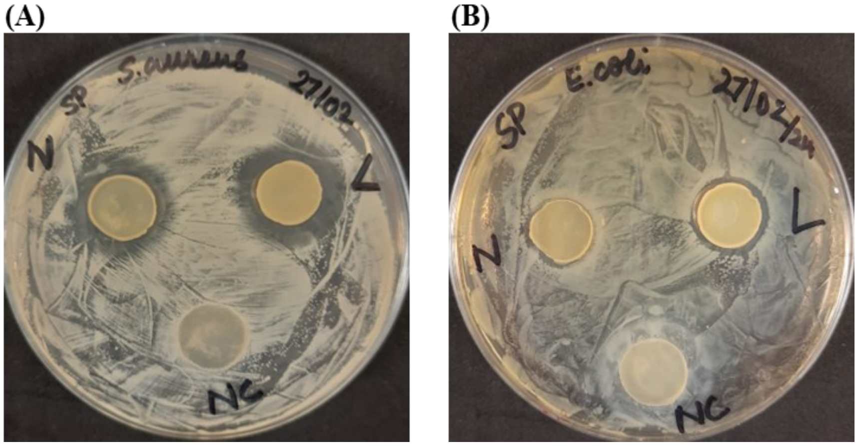

Figure 4.6 Antibacterial activity of OXCL-N (N), OXCL-L (L), and OXCL (NC) hydrogels against (A) *S. aureus* and (B) *E. coli.*

4.5 CONCLUSION

In the present study, antibacterial cellulose-based hydrogels configurated with a unique core-shell design were developed from waste cotton textiles using the NaOH/urea system, and then chemically conjugated with nisin and lysozyme. Based on FTIR analysis, successful oxidation of cellulose and the incorporation of antibacterial compounds through Schiff base reactions were confirmed. The SEM analysis, mechanical test, and water retention test revealed that OXCL-L and OXCL-N hydrogels possessed superior characteristics supporting food coolant application. Furthermore, quantitative assessment performed by the disc diffusion method confirmed the antibacterial efficacy of OXCL-N and OXCL-L hydrogels, indicating their effectiveness in combating against the bacterial pathogens. Henceforth, the novel antibacterial cellulose-based hydrogels derived from waste cotton textiles have the potential to address food spoilage issues caused by undesirable microbial contamination from the meltwater and enhance food storage and preservation practices.

4.6 REFERENCES

1. Schanes, K., Dobernig, K., & Gözet, B. (2018). Food waste matters-A systematic review of household food waste practices and their policy implications. *Journal of cleaner production*, *182*, 978-991.
2. Mc Carthy, U., Uysal, I., Badia-Melis, R., Mercier, S., O'Donnell, C., & Ktenioudaki, A. (2018). Global food security–Issues, challenges and technological solutions. *Trends in Food Science & Technology*, *77*, 11-20.
3. Elik, A., Yanik, D. K., Istanbullu, Y., Guzelsoy, N. A., Yavuz, A., & Gogus, F. (2019). Strategies to reduce post-harvest losses for fruits and vegetables. *Strategies*, *5*(3), 29-39.
4. Azeem, M. K., Islam, A., Khan, R. U., Rasool, A., Qureshi, M. A. U. R., Rizwan, M., ... & Rasheed, T. (2023). Eco-friendly three-dimensional hydrogels for sustainable agricultural applications: Current and future scenarios. *Polymers for Advanced Technologies*, *34*(9), 3046-3062.
5. Manzoor, A., Dar, A. H., Pandey, V. K., Shams, R., Khan, S., Panesar, P. S., ... & Khan, S. A. (2022). Recent insights into polysaccharide-based hydrogels and their potential applications in food sector: A review. *International Journal of Biological Macromolecules*, *213*, 987-1006.
6. Thivya, P., Akalya, S., & Sinija, V. R. (2022). A comprehensive review on cellulose-based hydrogel and its potential application in the food industry. *Applied Food Research*, *2*(2), 100161.
7. Ali, A., & Ahmed, S. (2018). Recent advances in edible polymer based hydrogels as a sustainable alternative to conventional polymers. *Journal of agricultural and food chemistry*, *66*(27), 6940-6967.

8. Bashari, A., Rouhani Shirvan, A., & Shakeri, M. (2018). Cellulose-based hydrogels for personal care products. *Polymers for Advanced Technologies*, *29*(12), 2853-2867.
9. Selvaraj, S., Chauhan, A., Dutta, V., Verma, R., Rao, S. K., Radhakrishnan, A., & Ghotekar, S. (2024). A state-of-the-art review on plant-derived cellulose-based green hydrogels and their multifunctional role in advanced biomedical applications. *International Journal of Biological Macromolecules*, 130991.
10. Ma, J., Liu, Y., Ali, O., Wei, Y., Zhang, S., Zhang, Y., ... & Luo, S. (2018). Fast adsorption of heavy metal ions by waste cotton fabrics based double network hydrogel and influencing factors insight. *Journal of hazardous materials*, *344*, 1034-1042.
11. Jirawitchalert, S., Mitaim, S., Chen, C. Y., & Patikarnmonthon, N. (2022). Cotton cellulose-derived hydrogel and electrospun fiber as alternative material for wound dressing application. *International Journal of Biomaterials*, *2022,* 12.
12. Gunes, O. C., & Ziylan Albayrak, A. (2021). Antibacterial Polypeptide nisin containing cotton modified hydrogel composite wound dressings. *Polymer Bulletin*, *78*(11), 6409-6428.
13. Wu, T., Huang, J., Jiang, Y., Hu, Y., Ye, X., Liu, D., & Chen, J. (2018). Formation of hydrogels based on chitosan/alginate for the delivery of lysozyme and their antibacterial activity. *Food chemistry*, *240*, 361-369.
14. Saini, S., Sillard, C., Belgacem, M. N., & Bras, J. (2016). Nisin anchored cellulose nanofibers for long term antimicrobial active food packaging. *RSC advances*, *6*(15), 12422-12430.

15. Sahu, S., & Pramanik, K. (2018). Evaluation and optimization of organic acid pretreatment of cotton gin waste for enzymatic hydrolysis and bioethanol production. *Applied biochemistry and biotechnology*, *186*(4), 1047-1060.
16. Chu, Y., Popovich, C., & Wang, Y. (2023). Heat sealable regenerated cellulose films enabled by zein coating for sustainable food packaging. Composites Part C: Open Access, 12, 100390.
17. Aarstad, O., Heggset, E.B., Pedersen, I.S., Bjørnøy, S.H., Syverud, K., Strand, B.L. (2017). Mechanical Properties of Composite Hydrogels of Alginate and Cellulose Nanofibrils. Polymers, 9, 378.
18. Abou-Yousef, H., Dacrory, S., Hasanin, M., Saber, E., & Kamel, S. (2021). Biocompatible hydrogel based on aldehyde-functionalized cellulose and chitosan for potential control drug release. *Sustainable Chemistry and Pharmacy*, *21*, 100419.
19. Zohri, M., Alavidjeh, M. S., Haririan, I., Ardestani, M. S., Ebrahimi, S. E. S., Sani, H. T., & Sadjadi, S. K. (2010). A comparative study between the antibacterial effect of nisin and nisin-loaded chitosan/alginate nanoparticles on the growth of Staphylococcus aureus in raw and pasteurized milk samples. *Probiotics and Antimicrobial proteins*, *2*, 258-266.
20. Odabaşi, M., Say, R., & Denizli, A. (2007). Molecular imprinted particles for lysozyme purification. *Materials Science and Engineering: C*, *27*(1), 90-99.
21. Mohd Rasid, N. H., Abdul Halid, N., Song, A. A. L., Sabri, S., Saari, N., & Hasan, H. (2023). Effects of individual and combined fermentation factors on antimicrobial activity of nisin by Lactococcus lactis ATCC 11454. *Molecular biotechnology*, *65*(6), 861-870.

22. Tafreshi, S. Y. H., Mirdamadi, S., & Khatami, S. (2020). Comparison of different nisin separation and concentration methods: Industrial and cost-effective perspectives. *Probiotics and antimicrobial proteins*, *12*, 1226-1234.
23. Diken Gür, S., Bakhshpour, M., Bereli, N., & Denizli, A. (2021). Antibacterial effect against both Gram-positive and Gram-negative bacteria via lysozyme imprinted cryogel membranes. *Journal of Biomaterials Science, Polymer Edition*, *32*(8), 1024-1039.
24. Yadollahi, M., Gholamali, I., Namazi, H., & Aghazadeh, M. (2015). Synthesis and characterization of antibacterial carboxymethyl cellulose/ZnO nanocomposite hydrogels. *International journal of biological macromolecules*, *74*, 136-141.
25. El-Naggar, M. E., Gaballah, S., Abdel-Maksoud, G., El-Sayed, H. S., & Youssef, A. M. (2022). Preparation of bactericidal zinc oxide nanoparticles loaded carboxymethyl cellulose/polyethylene glycol cryogel for gap filling of archaeological bones. *Journal of Materials Research and Technology*, *20*, 114-127.
26. Lopes, A. R. D. O., Locatelli, G. O., Barbosa, R. D. M., Lobo Junior, M., Moura Mascarin, G., & Lamenha Luna Finkler, C. (2020). Preparation, characterisation and cell viability of encapsulated Trichoderma asperellum in alginate beads. *Journal of Microencapsulation*, *37*(3), 270-282.
27. Vinceković, M., Šegota, S., Jurić, S., Harja, M., & Ondrasek, G. (2022). Development and characterization of a novel soil amendment based on biomass fly ash encapsulated in calcium alginate microspheres. *International journal of molecular sciences*, *23*(17), 9984.
28. Balkız, G., Pingo, E., Kahya, N., Kaygusuz, H., & Bedia Erim, F. (2018). Graphene oxide/alginate quasi-cryogels for removal of methylene blue. *Water, Air, & Soil Pollution*, *229*, 1-9.

29. Moravej, H., Moravej, Z., Yazdanparast, M., Heiat, M., Mirhosseini, A., Moosazadeh Moghaddam, M., & Mirnejad, R. (2018). Antimicrobial peptides: features, action, and their resistance mechanisms in bacteria. Microbial Drug Resistance, 24(6), 747-767.
30. Pérez-Ramos, A., Madi-Moussa, D., Coucheney, F., & Drider, D. (2021). Current knowledge of the mode of action and immunity mechanisms of LAB-bacteriocins. Microorganisms, 9(10), 2107.
31. Ferraboschi, P., Ciceri, S., & Grisenti, P. (2021). Applications of lysozyme, an innate immune defense factor, as an alternative antibiotic. Antibiotics, 10(12), 1534.
32. Abdulkhani, A., Najd Mazhar, A., Hedjazi, S., & Hamzeh, Y. (2020). Preparation of xylan bio-composite films reinforced with oxidized carboxymethyl cellulose and nanocellulose. *Polymer Bulletin*, *77*, 6227-6239.
33. Sheng, C., Zhou, Y., Lu, J., Zhang, X., & Xue, G. (2019). Preparation and characterization of chitosan based hydrogels chemical cross-linked by oxidized cellulose nanowhiskers. *Polymer Composites*, *40*(6), 2432-2440.
34. Sultana, N., Edlund, U., Guria, C., & Westman, G. (2024). Kinetics of periodate-mediated oxidation of cellulose. *Polymers*, *16*(3), 381.
35. Errokh, A., Magnin, A., Putaux, J. L., & Boufi, S. (2018). Morphology of the nanocellulose produced by periodate oxidation and reductive treatment of cellulose fibers. *Cellulose*, *25*, 3899-3911.
36. He, X., Li, Y., Zhang, L., Du, R., Dai, Y., & Tan, Z. (2021). Preparation of 2, 3-dialdehyde microcrystalline cellulose particles crosslinked with ε-poly-L-lysine and their antibacterial activity. *Cellulose*, *28*, 2833-2847.

37. Zhang, L., Yan, P., Li, Y., He, X., Dai, Y., & Tan, Z. (2020). Preparation and antibacterial activity of a cellulose-based Schiff base derived from dialdehyde cellulose and L-lysine. *Industrial Crops and Products*, *145*, 112126.
38. Milošević, J., Petrić, J., Jovčić, B., Janković, B., & Polović, N. (2020). Exploring the potential of infrared spectroscopy in qualitative and quantitative monitoring of ovalbumin amyloid fibrillation. *Spectrochimica Acta Part A: Molecular and Biomolecular Spectroscopy*, *229*, 117882.
39. Wu, H., Teng, C., Liu, B., Tian, H., & Wang, J. (2018). Characterization and long term antimicrobial activity of the nisin anchored cellulose films. *International journal of biological macromolecules*, *113*, 487-493.
40. Tavakolian, M., Okshevsky, M., van de Ven, T. G., & Tufenkji, N. (2018). Developing antibacterial nanocrystalline cellulose using natural antibacterial agents. *ACS applied materials & interfaces*, *10*(40), 33827-33838.
41. De France, K. J., Kummer, N., Ren, Q., Campioni, S., & Nyström, G. (2020). Assembly of cellulose nanocrystal–lysozyme composite films with varied lysozyme morphology. *Biomacromolecules*, *21*(12), 5139-5147.
42. Huang, Y., Yang, P., Yang, F., & Chang, C. (2021). Self-supported nanoporous lysozyme/nanocellulose membranes for multifunctional wastewater purification. *Journal of Membrane Science*, *635*, 119537.
43. Tan, Y., Wu, H., Xie, T., Chen, L., Hu, S., Tian, H., ... & Wang, J. (2020). Characterization and antibacterial effect of quaternized chitosan anchored cellulose beads. *International journal of biological macromolecules*, *155*, 1325-1332.

44. Gao, P., Cha, R., Luo, H., Xu, Y., Zhang, P., Han, L., ... & Jiang, X. (2022). Development of antimicrobial oxidized cellulose film for active food packaging. *Carbohydrate Polymers*, *278*, 118922.
45. Wu, Y., Li, Q., Zhang, X., Li, Y., Li, B., & Liu, S. (2019). Cellulose-based peptidopolysaccharides as cationic antimicrobial package films. *International journal of biological macromolecules*, *128*, 673-680.
46. Wang, B., Zhao, X., Duan, C., Li, J., Zeng, J., Xu, J., ... & Chen, K. (2023). Novel carboxylated cellulose nanocrystals synthesized by co-oxidation of sodium periodate/Fenton as a green solid emulsifier for oil-in-water Pickering emulsion. *Journal of Colloid and Interface Science*, *630*, 604-617.
47. Gong, F., Qian, J., Chen, Y., Yao, S., Tong, J., & Guo, H. (2018). Preparation and properties of gum arabic cross-link binding nisin microparticles. *Carbohydrate polymers*, *197*, 608-613.
48. Gao, G., Fan, H., Zhang, Y., Cao, Y., Li, T., Qiao, W., ... & Li, G. (2021). Production of nisin-containing bacterial cellulose nanomaterials with antimicrobial properties through co-culturing Enterobacter sp. FY-07 and Lactococcus lactis N8. *Carbohydrate Polymers*, *251*, 117131.
49. Lu, P., Zhao, H., Zheng, L., Duan, Y., Wu, M., Yu, X., & Yang, Y. (2022). Nanocellulose/nisin hydrogel microparticles as sustained antimicrobial coatings for paper packaging. *ACS Applied Polymer Materials*, *4*(4), 2664-2673.
50. Bayazidi, P., Almasi, H., & Asl, A. K. (2018). Immobilization of lysozyme on bacterial cellulose nanofibers: Characteristics, antimicrobial activity and morphological properties. *International journal of biological macromolecules*, *107*, 2544-2551.

51. Feng, S., Yi, J., Ma, Y., & Bi, J. (2023). Study on the ice crystals growth under pectin gels with different crosslinking strengths by modulating the degree of amidation in HG domain. *Food Chemistry*, *428*, 136758
52. Zhai, M., Ma, F., Li, J., Wan, B., & Yu, N. (2018). Preparation and properties of cryogel based on poly (hydroxypropyl methacrylate). *Journal of Biomaterials Science, Polymer Edition*, *29*(12), 1401-1425.
53. Guo, Y., Wu, M., Li, R., Cai, Z., & Zhang, H. (2022). Thermostable physically crosslinked cryogel from carboxymethylated konjac glucomannan fabricated by freeze-thawing. *Food Hydrocolloids*, *122*, 107103.
54. Yi, Y., Zhang, Y., Mansel, B., Wang, Y. N., Prabakar, S., & Shi, B. (2022). Effect of dialdehyde carboxymethyl cellulose cross-linking on the porous structure of the collagen matrix. *Biomacromolecules*, *23*(4), 1723-1732.
55. Ma, W., Yuan, C., Cui, B., Gao, T., Guo, L., Yu, B., ... & Zou, F. (2024). Highly-branched cyclic dextrin for improvement in mechanical properties and freeze-thaw stability of κ-carrageenan gels. *Food Hydrocolloids*, *148*, 109497.
56. Zhu, C., Zou, S., Rao, Z., Min, L., Liu, M., Liu, L., & Fan, L. (2017). Preparation and characterization of hydroxypropyl chitosan modified with nisin. *International journal of biological macromolecules*, *105*, 1017-1024.
57. Wu, Y., & Li, C. (2023). A double-layer smart film based on gellan gum/modified anthocyanin and sodium carboxymethyl cellulose/starch/Nisin for application in chicken breast. *International Journal of Biological Macromolecules*, *232*, 123464.

58. Diblan, S., Gökkaya Erdem, B., & Kaya, S. (2020). Sorption, diffusivity, permeability and mechanical properties of chitosan, potassium sorbate, or nisin incorporated active polymer films. *Journal of Food Science and Technology*, *57*, 3708-3719.
59. Xie, Y., Gong, W., Jin, J., Zhao, Z., Li, Z., & Zhou, J. (2020). Molecular simulations of lysozyme adsorption on an electrically responsive mixed self-assembled monolayer. *Applied Surface Science*, *506*, 144962.
60. Teixeira, M. C., Lameirinhas, N. S., Carvalho, J. P., Valente, B. F., Luís, J., Pires, L., ... & Freire, C. S. (2022). Alginate-lysozyme nanofibers hydrogels with improved rheological behavior, printability and biological properties for 3D bioprinting applications. *Nanomaterials*, *12*(13), 2190.
61. Morè, N., Martorana, A. M., Biboy, J., Otten, C., Winkle, M., Serrano, C. K. G., ... & Polissi, A. (2019). Peptidoglycan remodeling enables Escherichia coli to survive severe outer membrane assembly defect. MBio, *10*(1), 10-1128.
62. Leśnierowski, G., & Yang, T. (2021). Lysozyme and its modified forms: A critical appraisal of selected properties and potential. Trends in Food Science & Technology, *107*, 333-342.

CHAPTER 5. A COMPREHENSIVE SCHOLARLY DISCUSSION OF ALL THE FINDINGS

In this thesis, we developed novel cellulose-based hydrogels from the waste cotton textiles with a unique core-shell structure for the potential applications as food coolants. In Chapter 3, feasibility and suitability of the cellulose-based hydrogels as a food coolant were determined. This was done by characterizing the cellulose-based hydrogels for critical parameters such as their morphology, compressive strength, water retention capacity, reusability, and latent heat of fusion. Further, the cooling efficiency test was performed between the conventional ice cubes and C2A10Cl hydrogel by investigating their cooling curves using blueberries and thawing curves under controlled conditions. The results showed that the specialized core-shell structure of the hydrogels evidently influenced their compressive strength, water retention, and latent heat of fusion properties. The higher Ca^{2+} ion content in the coating layer was instrumental in offering a high protectiveness to the hydrogel, which could have aided in reducing the effect of mechanical stress in the core layer during the freeze-thaw treatments. Notably, CA2A10Cl hydrogels achieved the highest water-retention capacity of 97.4% after freeze-thaw cycle 1 and 88.8% after 5 cycles, while C2A10Cl exhibited the highest compressive strength of 144.7 kPa before freeze-thaw treatment and 87.1 kPa after freeze-thaw cycle 5 due to the high Ca^{2+} ion concentration in the coating solution. The latent heat of fusion of all the cellulose-based hydrogels was comparable to the conventional ice cubes even after freeze-thaw cycle 5. Particularly, C2A5Cl hydrogel demonstrated the highest latent heat of fusion of 305.9 J/g at freeze-thaw cycle 0 and with a slight decline to 273.3 J/g after 5 cycles. The comparative analysis was conducted between conventional ice cubes and C2A10Cl to study the thawing curves and cooling effectiveness on blueberries. The C2A10Cl hydrogel demonstrated similar thawing behavior in retaining and releasing thermal energy to the conventional ice cubes. Both conventional ice cubes and C2A10Cl hydrogel effectively cooled the blueberries to below 4°C within 26 mins and 32 mins, respectively. The notable cooling efficiency and high-water retention capacity of the C2A10Cl hydrogel suggested its potential for preserving the freshness of perishable foods while acting as a viable coolant. Further research is needed to optimize the hydrogel composition, enhance the cooling efficiency, and test for food preservation.

In Chapter 4, the aim was to reduce the susceptibility of microbial proliferation during food storage and transportation by applying antibacterial hydrogel coolants. Based on the findings of Chapter 3, the cellulose-based hydrogels were oxidized using sodium periodate and then combined with the GRAS approved antibacterial compounds, namely nisin and lysozyme, through Schiff base reaction. These hydrogels were characterized using fourier transform infrared spectroscopy, scanning electron microscopy, compressive strength test, water retention test, and disc diffusion assay. Nisin is a natural antibacterial peptide with regulatory approval in food applications due to the broad spectrum of antibacterial activity against gram-positive bacteria at low concentrations. Conversely, lysozyme is also a GRAS-safe natural enzyme, effective for food preservation with good heat stability and high potency against gram-positive bacteria. The water retention capacities of the OXCL-N (81.1%) and OXCL-L (80.2%) hydrogels were higher than OXCL hydrogels, which might be due to the hydrophilic nature of nisin and lysozyme. The cellulose-based hydrogels exhibited certain reusability after successive freeze-thaw cycles. The assessment of the mechanical properties of the hydrogels offered insights into the structural integrity and durability. The OXCL-N (142.8 kPa) and OXCL-L (127.1 kPa) hydrogels displayed higher compressive strengths than OXCL (116.6 kPa) hydrogel. It was due to the Schiff base reaction in which amine groups of antibacterial compounds bound with the aldehyde groups of cellulose-based hydrogels. After 1-freeze-thaw cycle, OXCL, OXCL-L, and OXCL-N hydrogels displayed the compressive strength of 28.9 kPa, 32.7 kPa, and 48.3 kPa, respectively. After 5 successive freeze-thaw cycles, improved stability of the OXCL (52.5 kPa), OXCL-N (79.1 kPa), and OXCL-L (92.6 kPa) hydrogels was observed, which might be due to the physical crosslinking, i.e., the growth of ice grains during freezing step and the subsequent polymer rearrangement during the melting process. To study the antibacterial properties of OXCL, OXCL-N, and OXCL-L hydrogels, a disc diffusion method was performed. The control sample, OXCL hydrogel displayed no antibacterial effect, but remarkably, the OXCL-N and OXCL-L hydrogels exhibited obvious inhibition zones measuring 3.66 mm and 4.06 mm against the Gram-positive bacteria, *S. aureus* respectively, confirming the successful antibacterial modification. Conversely, the relatively lower inhibition capacity against *E. coli* by OXCL-N (1.1 mm) and OXCL-L (1.2 mm) could be attributed to the existence of the outer membrane of Gram-negative bacteria.

On the other hand, certain limitations of the methodology employed for the development of cellulose-based hydrogels must be addressed. The sulfuric acid pretreatment should be well controlled. Optimizing the concentration of sulfuric acid and the duration of pretreatment is necessary to prevent excessive hydrolysis and over-degradation of cellulose that can impact the overall hydrogel-quality. Also, the residue of chemical crosslinker epichlorohydrin should be completely removed to ensure the safety in food contact applications.

Impact of this research

As per our knowledge, for the first time, this study reports the development of a food coolant system from a waste resource as a potential alternative to conventional coolants, hence contributing to global efforts in reducing waste and minimizing environmental impact by utilizing waste products and repurposing them into value-added products. Moreover, it also contributes to understanding the functional material design and its properties for improved performance. This study addresses the practical applications by assessing the stability and durability of the cellulose-based hydrogels over successive freeze-thaw cycles, and gave insights into the feasibility and performance of the hydrogels in sustained real-world applications. Further, comparative studies provided novel perspectives into the viability of the obtained hydrogels with no meltwater generation, while demonstrating similar cooling and thawing patterns with the conventional ice cubes. The antibacterial cellulose-based hydrogels could contribute to a better food safety practice by effectively preventing microbial contamination during food storage and transportation.

CHAPTER 6. GENERAL SUMMARY AND CONCLUSION

6.1 GENERAL SUMMARY

While the conventional ice cubes have numerous advantages such as high latent heat of fusion (334 J/g), non-toxicity, accessibility, and low cost, they have also caused problems such as cross-contamination of food products and excessive consumption of water. Therefore, it is imperative to develop a food coolant with excellent water retention ability sourced from renewable resources that can effectively reduce the contamination issues arising from meltwater. In the literature review, the preparation methods and various food-related industrial applications of cellulose hydrogels have been summarized. In particular, the synthesis of hydrogels using physical and chemical crosslinking techniques and their numerous applications in the fields of food industry, wastewater treatment, and sustainable agriculture were reviewed. Herein, we focused on the development of cellulose-based hydrogels with high performance from waste cotton textiles, using the NaOH/urea/water system, to address the meltwater-related cross-contamination issues. The results showed that the C2A10Cl hydrogels had good mechanical strength of 144.7 kPa, water retention capacity of 72.2%, and high latent heat of fusion of 272.5 J/g. The thawing curve of the C2A10Cl hydrogel displayed good similarity to the conventional ice cubes, observed over a period of 330 minutes, and the cooling behavior of C2A10Cl on blueberries was comparable to that of the conventional ice cubes. Furthermore, as cellulose is not inherently antibacterial in nature, nisin and lysozymes were incorporated into the cellulose-based hydrogels to endow them with antibacterial properties. The study on OXCL-L and OXCL-N hydrogels revealed the improved water retention capacity of 80.2% and 81.1% and the higher mechanical strength of 127.1 kPa and 142.8 KPa after the incorporation of antibacterial compounds. The antibacterial test demonstrated the zone of inhibition of 4.06 mm and 3.66 mm for OXCL-L and OXCL-N hydrogels against *S. aureus* respectively, as well as slight inhibition effect against the Gram-negative bacteria, *E.coli*.

6.2 SUGGESTIONS FOR FUTURE WORK

This study provides a promising approach for the development of cellulose-based hydrogels with a distinctive core-shell design that exhibit high performance and cooling efficiency. In particular, the exceptional mechanical strength, noteworthy latent heat of fusion, and high water retention ability offered the possibility of the cellulose-based hydrogels as a potential eco-friendly alternative. Since this research work focused mainly on the water retention, mechanical and thermal properties, and the reusability of cellulose-based hydrogels after consecutive freeze-thaw cycles, further research should focus on i) optimizing the dip-coating technique by involving various compositions for improved water absorption and retention properties, ii) taking into consideration the temperature conditions applied during freeze-thaw treatments for the improved structural integrity of hydrogels with repeated freeze-thaw cycles, iii) new strategies to enhance the water retention capacity of cellulose-based hydrogels, iv) aligning cooling and thawing kinetics of the hydrogels to that of the conventional ice cubes without any negative effects on the mechanical and latent heat of fusion characteristics; v) testing the antimicrobial activity for other types of bacteria, and vi) focusing on the compatibility of the hydrogel coolants with various food products along with a careful consideration of the consumer acceptance. Hence, it would be compelling to implement these cellulose hydrogel coolants in real-life applications to further optimize the coolant technology, ultimately aiming for a safe and sustainable food system with reduced microbial contaminations.

REFERENCES

1. Sarwar, T., & Khan, S. (2022). Textile industry: pollution health risks and toxicity. In *Textile Wastewater Treatment: Sustainable Bio-nano Materials and Macromolecules, Volume 1* (pp. 1-28). Singapore: Springer Nature Singapore.

2. Atkar, A., Pabba, M., Sekhar, S. C., & Sridhar, S. (2021). Current limitations and challenges in the global textile sector. In *Fundamentals of Natural Fibres and Textiles* (pp. 741-764). Woodhead Publishing.

3. Abbate, S., Centobelli, P., Cerchione, R., Nadeem, S. P., & Riccio, E. (2024). Sustainability trends and gaps in the textile, apparel and fashion industries. *Environment, Development and Sustainability*, *26*(2), 2837-2864.

4. Pensupa, N., Leu, S. Y., Hu, Y., Du, C., Liu, H., Jing, H., ... & Lin, C. S. K. (2018). Recent trends in sustainable textile waste recycling methods: current situation and future prospects. *Chemistry and Chemical Technologies in Waste Valorization*, *375(5),* 76.

5. Khan, M. A., Wahid, A., Ahmad, M., Tahir, M. T., Ahmed, M., Ahmad, S., & Hasanuzzaman, M. (2020). World cotton production and consumption: An overview. *Cotton production and uses: Agronomy, crop protection, and postharvest technologies*, *Chapter 1,* 1-7.

6. Huang, X., Tan, Y., Huang, J., Zhu, G., Yin, R., Tao, X., & Tian, X. (2024). Industrialization of open-and closed-loop waste textiles recycling towards sustainability: A review. *Journal of Cleaner Production*, 140676.

7. Zhou, Q., Le, Q. V., Meng, L., Yang, H., Gu, H., Yang, Y., ... & Peng, W. (2022). Environmental perspectives of textile waste, environmental pollution and recycling. *Environmental Technology Reviews*, *11*(1), 62-71.

8. Hossain, L., Sarker, S. K., & Khan, M. S. (2018). Evaluation of present and future wastewater impacts of textile dyeing industries in Bangladesh. *Environmental Development*, *26*, 23-33.

9. Kasavan, S., Yusoff, S., Guan, N. C., Zaman, N. S. K., & Fakri, M. F. R. (2021). Global trends of textile waste research from 2005 to 2020 using bibliometric analysis. *Environmental Science and Pollution Research*, *28*, 44780-44794.

10. John, E. P., & Mishra, U. (2023). A sustainable three-layer circular economic model with controllable waste, emission, and wastewater from the textile and fashion industry. *Journal of cleaner production*, *388*, 135642.

11. Yalcin-Enis, I., Kucukali-Ozturk, M., & Sezgin, H. (2019). Risks and management of textile waste. *Nanoscience and biotechnology for environmental applications*, *Chapter 2,* 29-53.

12. Shirvanimoghaddam, K., Motamed, B., Ramakrishna, S., & Naebe, M. (2020). Death by waste: Fashion and textile circular economy case. *Science of the total environment*, *718*, 137317.

13. Liu, W., Liu, S., Liu, T., Liu, T., Zhang, J., & Liu, H. (2019). Eco-friendly post-consumer cotton waste recycling for regenerated cellulose fibers. *Carbohydrate polymers*, *206*, 141-148.

14. Kale, R. D., Bansal, P. S., & Gorade, V. G. (2018). Extraction of microcrystalline cellulose from cotton sliver and its comparison with commercial microcrystalline cellulose. *Journal of Polymers and the Environment*, *26*, 355-364.

15. Zainal, S. H., Mohd, N. H., Suhaili, N., Anuar, F. H., Lazim, A. M., & Othaman, R. (2021). Preparation of cellulose-based hydrogel: A review. *Journal of Materials Research and Technology*, *10*, 935-952.

16. Zhou, L., Ke, K., Yang, M. B., & Yang, W. (2021). Recent progress on chemical modification of cellulose for high mechanical-performance Poly (lactic acid)/Cellulose composite: A review. *Composites Communications*, *23*, 100548.

17. Ndraha, N., Vlajic, J., Chang, C. C., & Hsiao, H. I. (2020). Challenges with food waste management in the food cold chains. In *Food industry wastes* (pp. 467-483). Academic Press.

18. Göransson, M., Nilsson, F., & Jevinger, Å. (2018). Temperature performance and food shelf-life accuracy in cold food supply chains–Insights from multiple field studies. *Food Control*, *86*, 332-341.

19. Skawińska, E., & Zalewski, R. I. (2022). Economic impact of temperature control during food transportation—A COVID-19 perspective. *Foods*, *11*(3), 467.

20. Karanth, S., Feng, S., Patra, D., & Pradhan, A. K. (2023). Linking microbial contamination to food spoilage and food waste: the role of smart packaging, spoilage risk assessments, and date labeling. *Frontiers in Microbiology*, *14*, 1198124.

21. Brenes, A. L. M., Brown, W., Steinmaus, S., Brecht, J. K., Xie, Y., Bornhorst, E. R., ... & Vorst, K. (2020). Temperature profiling of open-and closed-doored produce cases in retail grocery stores. *Food Control*, *113*, 107158.

22. Ricci, A., Martelli, F., Razzano, R., Cassi, D., Lazzi, C., Neviani, E., & Bernini, V. (2020). Service temperature preservation approach for food safety: microbiological evaluation of ready meals. *Food Control*, *115*, 107297.

23. Yahya, H. N., Lignou, S., Wagstaff, C., & Bell, L. (2019). Changes in bacterial loads, gas composition, volatile organic compounds, and glucosinolates of fresh bagged Ready-To-Eat rocket under different shelf life treatment scenarios. *Postharvest biology and technology*, *148*, 107-119.

24. Grace, D., & Fetsch, A. (2018). Staphylococcus aureus—A foodborne pathogen: Epidemiology, detection, characterization, prevention, and control: An overview. *Staphylococcus aureus*, *Chapter 1,* 3-10.

25. Xu, Z., Luo, Y., Mao, Y., Peng, R., Chen, J., Soteyome, T., ... & Kjellerup, B. V. (2020). Spoilage lactic acid bacteria in the brewing industry. *Journal of microbiology and biotechnology*, *30*(7), 955.

26. Ma, Y., Ding, S., Fei, Y., Liu, G., Jang, H., & Fang, J. (2019). Antimicrobial activity of anthocyanins and catechins against foodborne pathogens Escherichia coli and Salmonella. *Food Control*, *106*, 106712.

27. Luna-Guevara, J. J., Arenas-Hernandez, M. M., Martínez de la Peña, C., Silva, J. L., & Luna-Guevara, M. L. (2019). The role of pathogenic E. coli in fresh vegetables: Behavior,

contamination factors, and preventive measures. *International journal of microbiology*, *2019*, 2894328.

28. Zheng, Y., Ma, Y., Ukwatta, R. H., Xue, F., & Li, C. (2024). Development of Novel Cornstarch Hydrogel-Based Food Coolant and its Characterization. *Polymers*, *16*(5), 569.

29. Zou, J., Wang, L., & Sun, G. (2021). Sustainable and reusable gelatin-based hydrogel "jelly ice cubes" as food coolant. I: feasibilities and challenges. *ACS Sustainable Chemistry & Engineering*, *9*(46), 15357-15364.

30. Zou, J., Wang, L., & Sun, G. (2023). Mechanisms and Performances of Physically and Chemically Crosslinked Gelatin-Based Hydrogels as Advanced Sustainable and Reusable "Jelly Ice Cube" Coolants. *ACS Applied Materials & Interfaces*, *15*(28), 34087-34096.